TABLE 1
The IC_{50} values for the inhibitory effect of PGE_2 and $EP_{2/4}$ receptor agonists in the presence of AGE-2 and AGE-3
The results are expressed as the means ± S.E.M. of five donors with triplicate determinations.

	ICAM-1	B7.1	B7.2	CD40	TNF-α	IFN-γ	Proliferation
				nM			
AGE-2							
PGE_2	7 ± 0.2	7 ± 0.2	8 ± 0.3	8 ± 0.2	7 ± 0.2	8 ± 0.3	7 ± 0.3
ONO-AE1-259-01	9 ± 0.2	10 ± 0.1	10 ± 0.1	8 ± 0.3	7 ± 0.2	8 ± 0.2	7 ± 0.2
ONO-AE1-329	9 ± 0.2	10 ± 0.2	10 ± 0.1	10 ± 0.2	10 ± 0.2	10 ± 0.2	10 ± 0.3
AGE-3							
PGE_2	8 ± 0.3	8 ± 0.1	10 ± 0.2	15 ± 0.3	8 ± 0.3	8 ± 0.1	7 ± 0.4
ONO-AE1-259-01	8 ± 0.2	10 ± 0.1	10 ± 0.2	8 ± 0.2	7 ± 0.2	8 ± 0.2	8 ± 0.2
ONO-AE1-329	9 ± 0.2	10 ± 0.1	10 ± 0.2	10 ± 0.1	10 ± 0.3	10 ± 0.1	10 ± 0.2

lular adhesion molecule (ICAM)-1, B7, and CD40, on monocytes results in the activation of T cells (Durie et al., 1994; Ranger et al., 1996; Camacho et al., 2001). We also found that cell-to-cell interactions were brought about via the engagement between ICAM-1, B7.1, B7.2, and CD40 on monocytes and their ligands; lymphocyte function-associated antigen 1, CD28, and CD40 ligand on T cells were involved in T-cell activation, inducing the production of TNF-α and interferon (IFN)-γ in peripheral blood mononuclear cells (PBMC) (Takahashi et al., 2003). Blockade of the engagement of adhesion molecules by antibodies against ICAM-1, B7.1, B7.2, and CD40 reduced cytokine production in PBMC. In a previous study, we found that AGE-2 and AGE-3, but not AGE-4 and AGE-5, induced the expressions of ICAM-1, B7.1, B7.2, and CD40 on monocytes, the production of IFN-γ and TNF-α, and the lymphocyte proliferation in PBMC (Takahashi et al., 2009; Wake et al., 2009). We suggested that the activation of T cells by the enhancement of adhesion molecule expression on monocytes might result in the development of diabetic microangiopathy.

Prostaglandin E_2 (PGE_2), one of the major products of cyclooxygenase (COX)-initiated arachidonic acid metabolite released from monocytes, primes naive human T cells for enhanced production of anti-inflammatory cytokines and the inhibition of proinflammatory cytokines through COX-2 (Coleman et al., 1994; Hempel et al., 1994). There are four subtypes of PGE_2 receptors: prostanoid EP_1, EP_2, EP_3, and EP_4 receptors (Coleman et al., 1994). Activation of EP_2 and EP_4 receptors leads to an increase in cAMP levels (Coleman et al., 1994). However, little is known about the effect of PGE_2 on the AGE-2- and AGE-3-induced adhesion molecule expressions on monocytes. Therefore, we examined the effect of PGE_2 on AGE-2- and AGE-3-induced expressions of ICAM-1, B7.1, B7.2, and CD40 on monocytes, the production of IFN-γ and TNF-α, and the lymphocyte proliferation in PBMC.

Materials and Methods

Reagents and Drugs. PGE_2, AH6809, and AH23848 were purchased from Sigma-Aldrich (St. Louis, MO). ONO-D1-004, ONO-AE1-259-01, ONO-AE-248, ONO-AE1-329, and 11-deoxy-PGE_1 were provided by Ono Pharmaceutical Co. Ltd. (Tokyo, Japan). Glyceraldehyde-derived AGE (AGE-2) and glycolaldehyde-derived AGE (AGE-3) were prepared as described previously (Cuccurullo et al., 2006). In brief, AGE-bovine serum albumin (BSA) was prepared by incubating BSA at 50 mg/ml (Sigma-Aldrich) in $NaPO_4$ buffer (0.2 M, pH 7.4) with D-glyceraldehyde (AGE-2) at 0.2 M and D-glycolaldehyde (AGE-3) at 0.2 M (Wako, Tokyo, Japan) at 37°C for 7 days in the presence of 1.5 mM phenylmethylsulfonyl fluoride, 1 mM EDTA, and 1.0×10^5 U/l penicillin under endotoxin-free conditions. Dibutyryl cAMP (dbcAMP) and forskolin were purchased from Wako. H89 was purchased from Sigma-Aldrich. For flow cytometric analysis, a fluorescein isothiocyanate (FITC)-conjugated mouse IgG1 monoclonal antibody (mAb) against ICAM-1/CD54 was purchased from Dako Denmark A/S (Glostrup, Denmark). FITC-conjugated mouse IgG1 mAbs against B7.2 and CD40 were purchased from BD Pharmingen (San Diego, CA), and an FITC-conjugated IgG1 isotype-matched control was obtained from Sigma-Aldrich.

Isolation of PBMC and Monocytes. Normal human PBMCs were obtained from 10 healthy volunteers after acquiring institutional review board approval (Okayama University Institutional Review Board Number 106). Samples of 20 to 50 ml of peripheral blood were withdrawn from a forearm vein, after which PBMCs were prepared, and monocytes isolated from PBMC were separated by counterflow centrifugal elutriation as described previously (Takahashi et al., 2003). The PBMC and monocytes were then suspended at a final concentration of 1×10^6 cells/ml in the medium as described previously (Takahashi et al., 2003).

Flow Cytometric Analysis. Changes in the expression of human leukocyte antigens ICAM-1, B7.1, B7.2, and CD40 on monocytes were examined by multicolor flow cytometry using a combination of anti-CD14 Ab with anti-ICAM-1, anti-B7.1, anti-B7.2, or anti-CD40 Ab. PBMCs at 1×10^6 cells/ml were incubated for 24 h. Cultured cells at 5×10^5 cells/ml were prepared for flow cytometric analysis as previously described (Takahashi et al., 2003) and analyzed with a FACSCalibur (BD Biosciences, San Jose, CA). The data were processed using the CellQuest program (BD Biosciences).

Cytokine Assay. PBMCs at 1×10^6 cells/ml were used to analyze IFN-γ and TNF-α production. After culturing for 24 h at 37°C in a 5% CO_2/air mixture, cell-free supernatant was assayed for IFN-γ and TNF-α protein by enzyme-linked immunosorbent assay (ELISA) using the multiple Abs sandwich principle (R&D Systems, Minneapolis, MN). The detection limits of ELISA for IFN-γ and TNF-α were 10 pg/ml.

Proliferation Assay. PBMCs were treated with various conditions. Cultures were incubated for 48 h, during which they were pulsed with [^{3}H]thymidine (3 · 3 Ci/well) for the final 16 h. Cells were then divided into 96-well microplates, 200 μl/well, resulting in 1 μCi [^{3}H]thymidine per well, and harvested by the Micro-Mate 196 Cell Harvester (PerkinElmer Life and Analytical Sciences, Waltham, MA). Thymidine incorporation was measured by a beta-counter (Matrix 9600; PerkinElmer Life and Analytical Sciences).

Measurement of cAMP Production in Monocytes. Monocytes at 1×10^6 cells/ml were incubated at 37°C in a 5% CO_2/air mixture under different conditions. After the indicated periods, cells at 2×10^5 cells/200 μl/well were supplemented with trichloroacetic acid to a final concentration of 5% and 3-isobutyl-1-methylxanthine, an inhibitor of phosphodiesterase, at 100 μM and frozen at −80°C. Frozen samples were subsequently sonicated and assayed for cAMP using a cAMP enzyme immunoassay kit (Cayman Chemical, Ann

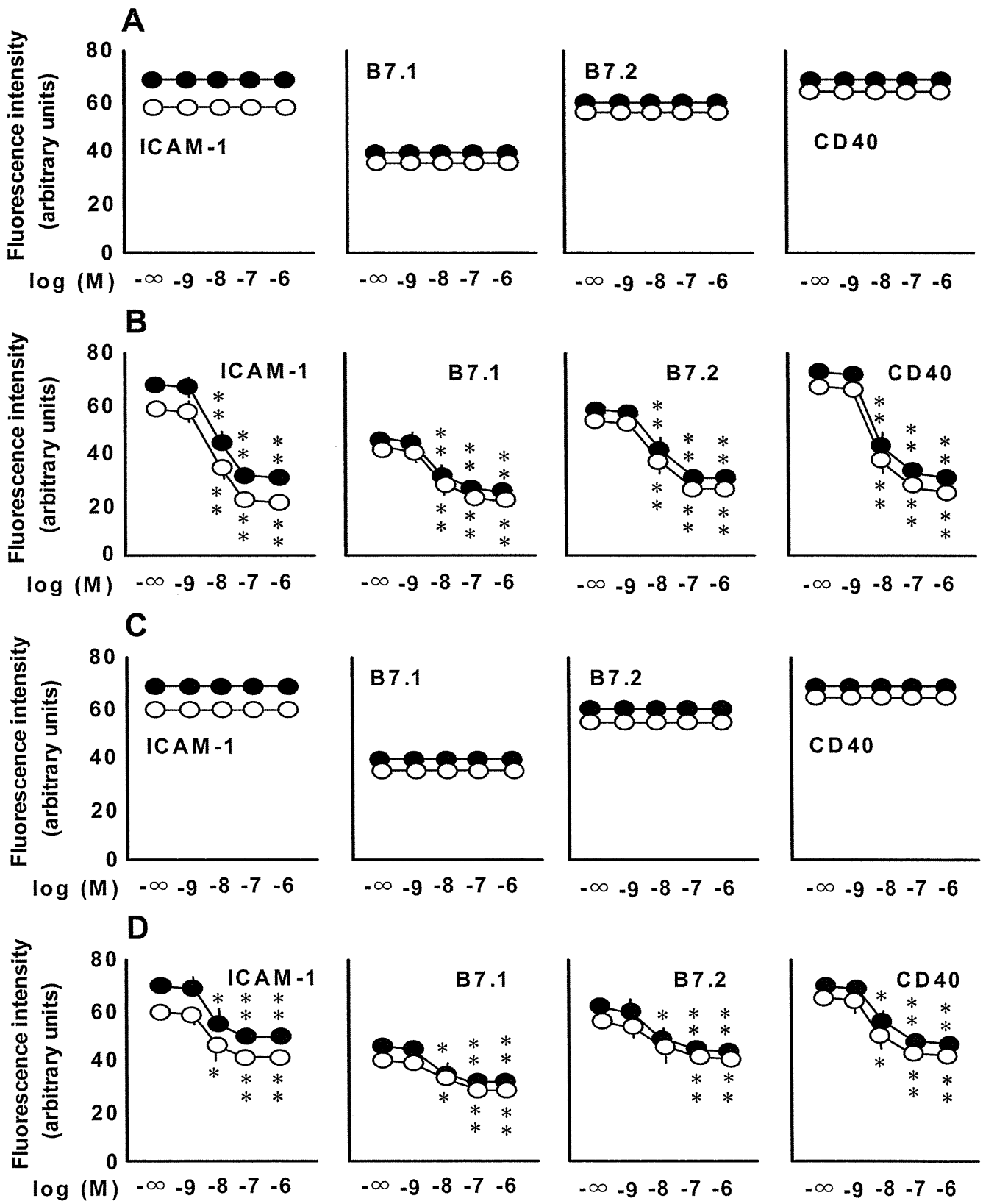

Fig. 3. The effect of prostanoid receptor agonists on AGE-2- and AGE-3-induced expressions of ICAM-1, B7.1, B7.2, and CD40 PBMC at 1×10^6 cells/ml was incubated with the EP_1 receptor agonist, ONO-D1-004 (A), the EP_2 receptor agonist, ONO-AE1-259-01 (B), the EP_3 receptor agonist, ONO-AE-248 (C), and the EP_4-receptor agonist, ONO-AE1-329 (D), at increasing concentrations from 1 nM to 1 μM in the presence of AGE-2 (filled circles; ●) and AGE-3 (open circles; ○) at 100 μg/ml for 24 h. The expressions of ICAM-1, B7.1, B7.2, and CD40 on monocytes were determined by flow cytometry. The results are expressed as the means ± S.E.M. of five donors with triplicate determinations. *, $P < 0.05$, **, $P < 0.01$ compared with the value for AGE-2 and AGE-3. When an error bar was within a symbol, the bar was omitted.

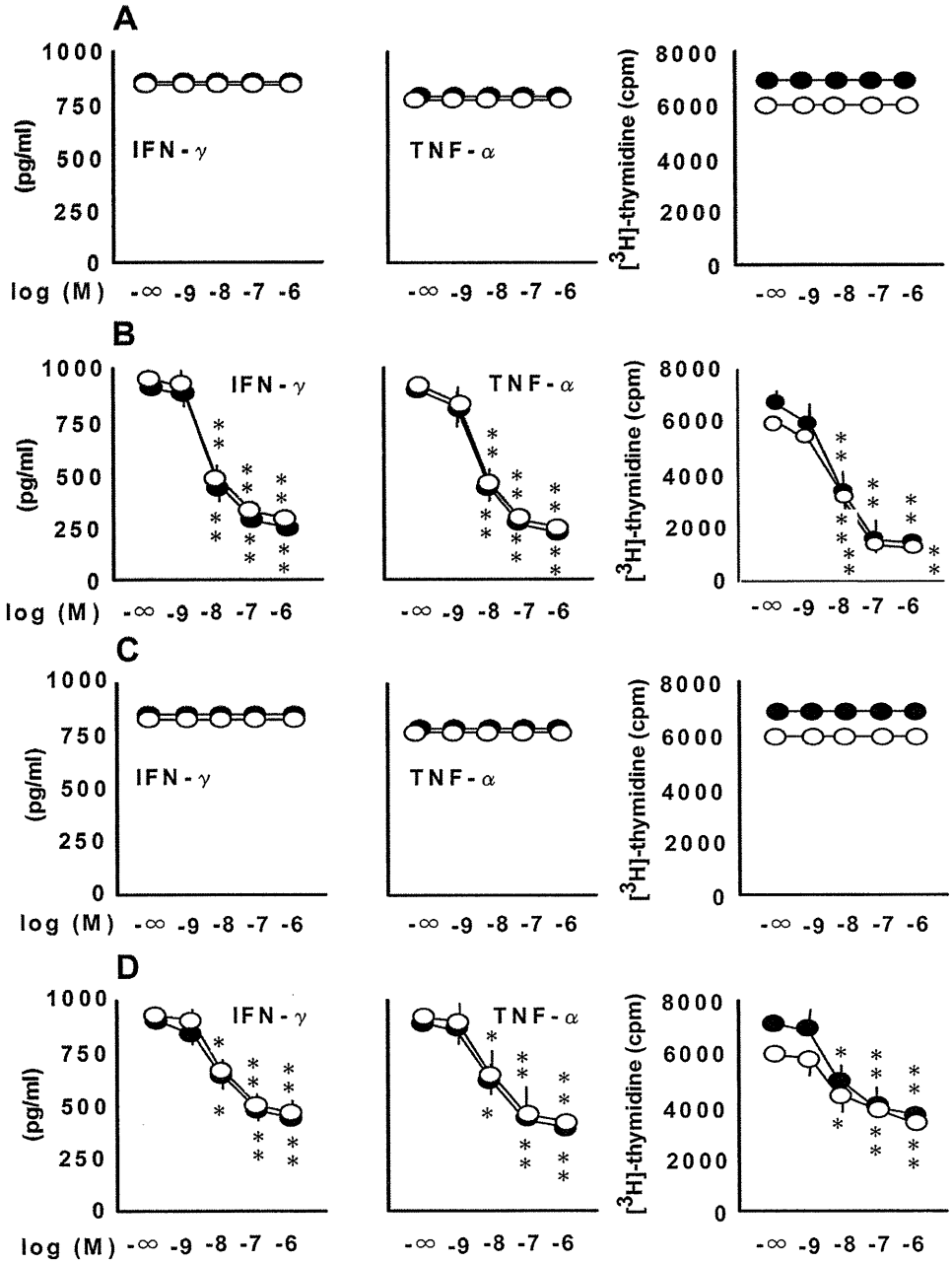

Fig. 4. The effect of prostanoid receptor agonists on AGE-2- and AGE-3-induced production of IFN-γ and TNF-α and the lymphocyte proliferation PBMC at 1×10^6 cells/ml were incubated with the EP_1 receptor agonist, ONO-D1-004 (A), the EP_2 receptor agonist, ONO-AE1-259-01 (B), the EP_3 receptor agonist, ONO-AE-248 (C), and the EP_4 receptor agonist, ONO-AE1-329 (D), at increasing concentrations from 1 nM to 1 μM in the presence of AGE-2 (filled circles; ●) and AGE-3 (open circles; ○) at 100 μg/ml for 24 h. IFN-γ and TNF-α concentrations in conditioned media were determined by ELISA. The lymphocyte proliferation was determined by [^{3}H]thymidine uptake as described under *Materials and Methods*. The results are expressed as the means ± S.E.M. of five donors with triplicate determinations. *, $P < 0.05$, **, $P < 0.01$ compared with the values for AGE-2 and AGE-3. When an error bar was within a symbol, the bar was omitted.

Arbor, MI) according to the manufacturer's instructions, for which no acetylation procedures were performed.

Statistical Examination. Statistical significance was evaluated using analysis of variance followed by Dunnett's test. A probability value of less than 0.05 was considered to indicate statistical significance. The results were expressed as the means ± S.E.M. of triplicate findings from five donors.

Results

Effects of PGE_2 on AGE-2- and AGE-3-Induced Expressions of ICAM-1, B7.1, B7.2, and CD40 on Monocytes, the Production of IFN-γ and TNF-α, and the Lymphocyte Proliferation in PBMC. In the previous study, to evaluate the binding of AGE subtypes to RAGE, we established an in vitro assay by using the immobilized AGE subspecies and the His-tagged soluble form of RAGE (sRAGE) protein (Takahashi et al., 2009). AGE-2 and AGE-3 showed relatively high affinity binding for sRAGE, whereas AGE-4 and AGE-5 showed moderate affinity for sRAGE. The appropriate incubation time and concentration of AGEs were determined according to the study (Takahashi et al., 2009; Wake et al., 2009). AGE-2 and AGE-3 at 100 μg/ml significantly induced the expressions of ICAM-1, B7.1, B7.2, and CD40, the production of IFN-γ and TNF-α, and the proliferation at 16 h and thereafter up to 24 and 48 h. Moreover, the effects of AGE-2 and AGE-3 at concentrations ranging from 100 ng/ml to 100 μg/ml for 24 h were determined. AGE-2 and AGE-3 at 10 and 100 μg/ml significantly induced the expressions of adhesion molecule, the cytokine production, and the lymphocyte proliferation.

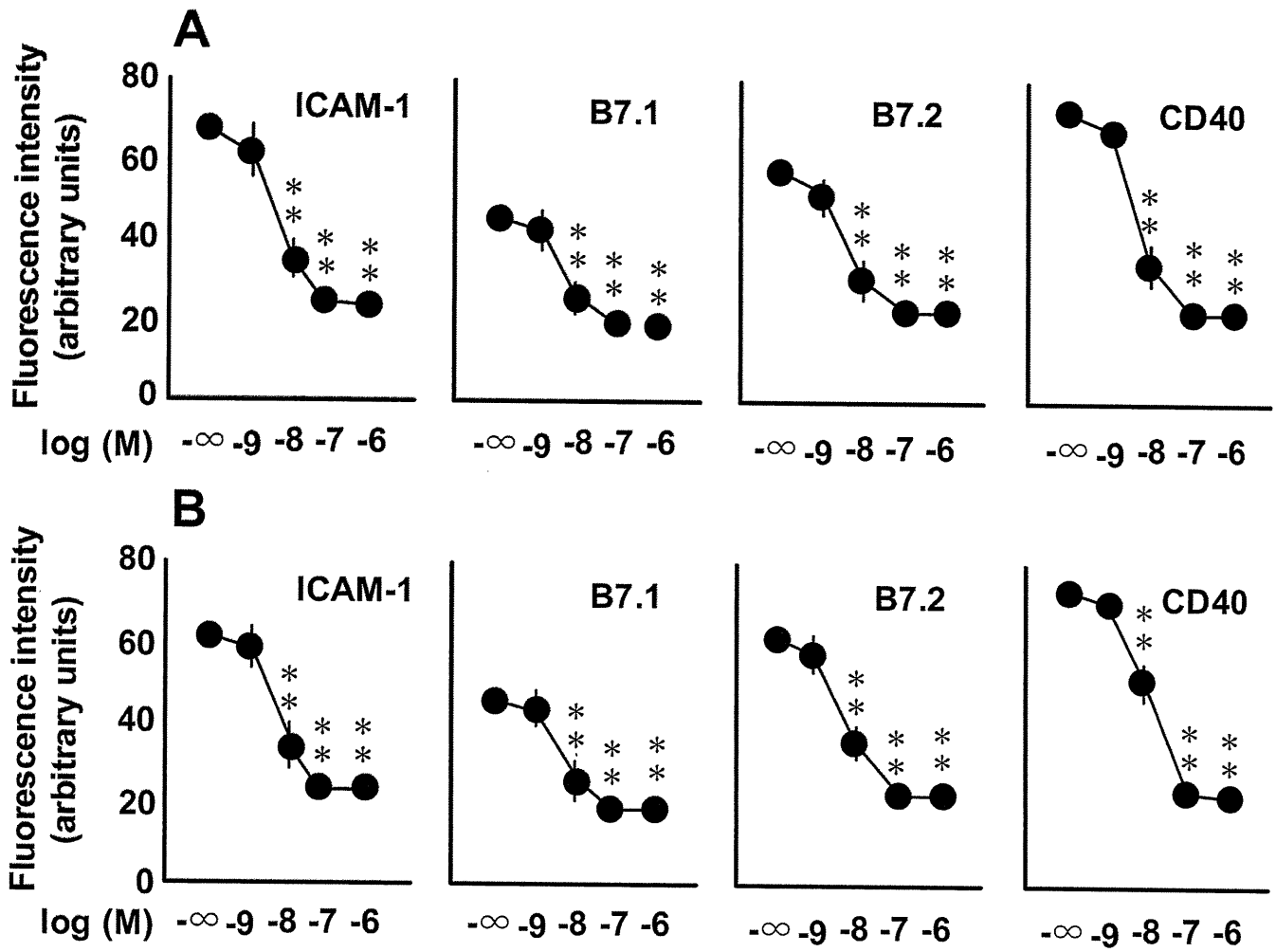

Fig. 5. The effects of 11-deoxy-PGE_1 on AGE-2- and AGE-3-induced ICAM-1, B7.1, B7.2, and CD40 expressions on human monocytes. PBMCs at 1×10^6 cells/ml were incubated with increasing concentrations of the EP_2/EP_4 receptor agonist, 11-deoxy-PGE_1 at increasing concentrations from 1 nM to 1 μM in the presence of AGE-2 (A) and AGE-3 (B) at 100 μg/ml for 24 h. The expressions of ICAM-1, B7.1, B7.2, and CD40 on monocytes were determined by flow cytometry. The results are expressed as the means ± S.E.M. of five donors with triplicate determinations. **, $P < 0.01$ compared with the values for AGE-2 and AGE-3. When an error bar was within a symbol, the bar was omitted.

As shown in Figs. 1 and 2, we established the effect of PGE_2 at concentrations ranging from 1 nM to 1 μM on the expressions of ICAM-1, B7.1, B7.2, and CD40 and its affect on the production of IFN-γ and TNF-α and the lymphocyte proliferation in the presence of AGE-2 and AGE-3 at 100 μg/ml. PGE_2 concentration-dependently inhibited AGE-2- and AGE-3-induced expressions of ICAM-1, B7.1, B7.2, and CD40, the production of IFN-γ and TNF-α, and the lymphocyte proliferation. The IC_{50} values for the inhibitory effect of PGE_2 on the expressions of ICAM-1, B7.1, B7.2, and CD40 and its affect on the production of IFN-γ and TNF-α and the lymphocyte proliferation in the presence of AGE-2 and AGE-3 are shown in Table 1. Moreover, we found that PGE_2 had no effect on the adhesion molecule expression and cytokine production in the presence of AGE-4 and AGE-5 (data not shown).

Involvement of Prostanoid EP_2 and EP_4 Receptors in the Actions of PGE_2. To determine the involvement of PGE_2 receptor subtypes in the effects of PGE_2 on the expressions of ICAM-1, B7.1, B7.2, and CD40, the production of IFN-γ and TNF-α, and the lymphocyte proliferation, the effects of an EP_1 receptor agonist, ONO-D1-004 (Suzawa et al., 2000; Noguchi et al., 2001), an EP_2 receptor agonist, ONO-AE1-259-01 (Suzawa et al., 2000; Noguchi et al., 2001), an EP_3 receptor agonist, ONO-AE-248 (Suzawa et al., 2000; Noguchi et al., 2001), and an EP_4 receptor agonist, ONO-AE1-329 (Suzawa et al., 2000; Noguchi et al., 2001), at concentrations ranging from 1 nM to 1 μM, on the adhesion molecule expression, the cytokine production, and the lymphocyte proliferation in the presence of AGE-2 and AGE-3 at 100 μM were determined (Figs. 3 and 4). The IC_{50} values for the inhibitory effect of ONO-AE1-259-01 and ONO-AE1-329 on the expressions of ICAM-1, B7.1, B7.2, and CD40 and its affect on the production of IFN-γ and TNF-α and the lymphocyte proliferation in the presence of AGE-2 and AGE-3 were shown in Table 1. It is apparent that the EP_2 and EP_4 receptor agonists concentration-dependently inhibited AGE-2- and AGE-3-induced effects on the adhesion molecule expression, the cytokine production, and the lymphocyte proliferation, but EP_1 and EP_3 receptor agonists had no effect. Moreover, we confirmed that a mixed EP_2/EP_4 receptor agonist, 11-deoxy-PGE_1 (Suzawa et al., 2000; Noguchi et al.,

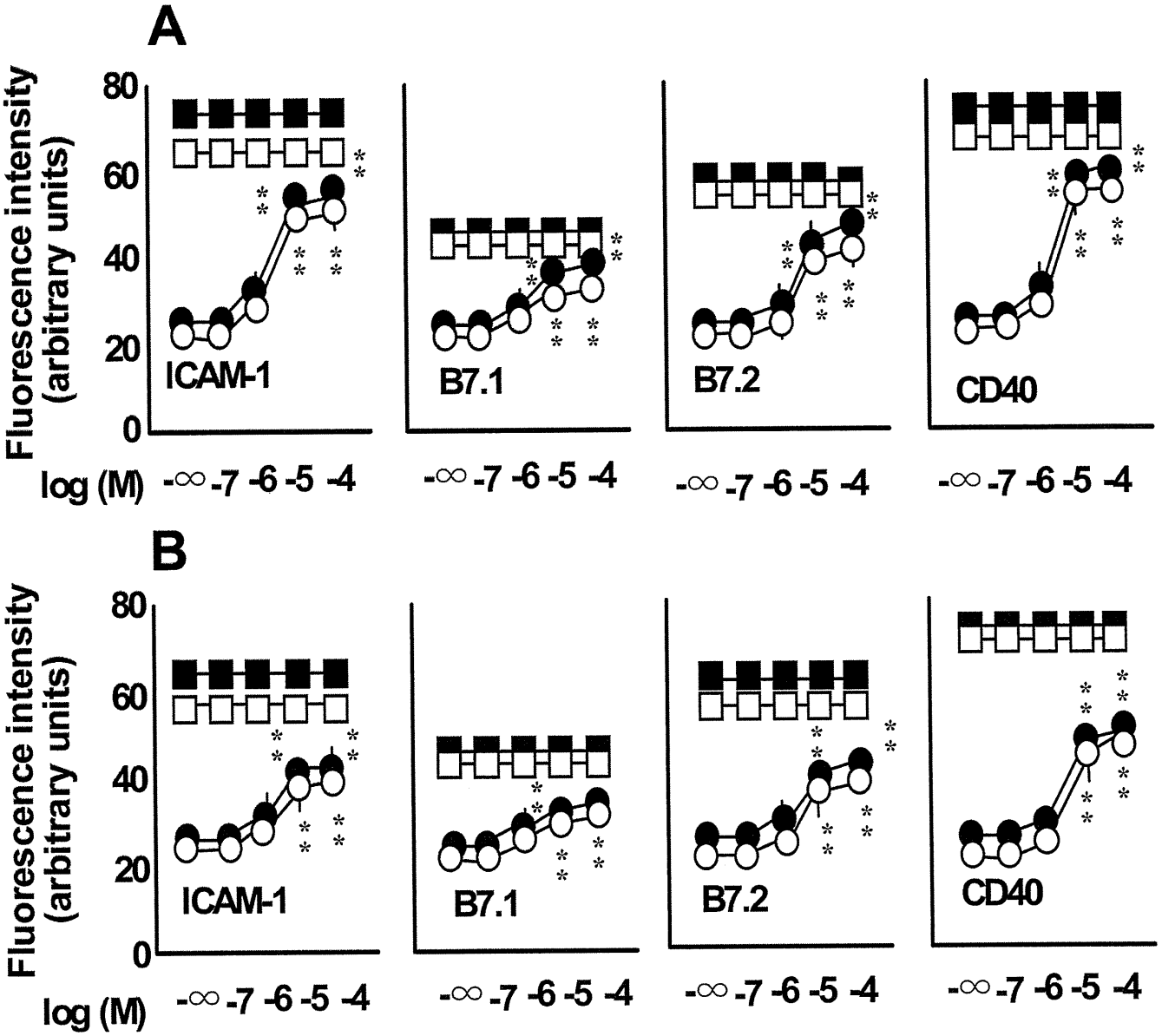

Fig. 6. The effects of prostanoid receptor antagonists on the inhibitory effect of PGE_2 on the expressions of ICAM-1, B7.1, B7.2, and CD40 PBMC at 1×10^6 cells/ml treated with PGE_2 at 1 μM were incubated with the EP_2 receptor antagonist, AH6809 (A), and the EP_4 receptor antagonist, AH23848 (B), at increasing concentrations from 0.1 to 100 μM in the presence of AGE-2 and AGE-3 at 100 μg/ml. The expressions of ICAM-1, B7.1, B7.2, and CD40 on monocytes were determined by flow cytometry. Filled circles (●) represent the effect of antagonists on PGE_2-inhibited adhesion molecule expression in the presence of AGE-2. Open circles (○) represent the effect of antagonists on PGE_2-inhibited adhesion molecule expression in the presence of AGE-3. Filled squares (■) represent the effect of antagonists on the actions of AGE-2 in the absence of PGE_2. Open squares (□) represent the effect of antagonists on the actions of AGE-3 in the absence of PGE_2. The results are expressed as the means ± S.E.M. of five donors with triplicate determinations. **, $P < 0.01$ compared with the values for PGE_2 in the presence of AGE-2 and AGE-3. When an error bar was within a symbol, the bar was omitted.

2001), inhibited AGE-2- and AGE-3-induced adhesion molecule expression in a concentration-dependent manner (Fig. 5). Moreover, the effect of an EP_2 receptor antagonist, AH6809 (Kay et al., 2006), and an EP_4 receptor antagonist, AH23848 (Kay et al., 2006), at concentrations ranging from 0.1 to 100 μM, on the adhesion molecule expression, cytokine production, and lymphocyte proliferation was examined in the presence of PGE_2 at 1 μM (Figs. 6 and 7). AH6809 and AH23848 reversed the inhibitory effect of PGE_2 on AGE-2- and AGE-3-induced expressions of ICAM-1, B7.1, B7.2, and CD40, the production of IFN-γ and TNF-α, and the lymphocyte proliferation in a concentration-dependent manner. On the other hand, AH6809 and AH23848 had no effect on the actions of AGE-2 and AGE-3 in the absence of PGE_2.

Effects of PGE_2 on the Production of cAMP in Monocytes in the Presence or Absence of AGE-2 and AGE-3. The effects of PGE_2 at 10 nM on the production of intracellular cAMP in monocytes isolated from PBMC in the presence (100 μg/ml) or absence of AGE-2 and AGE-3 were determined (Fig. 8). PGE_2 induced the production of cAMP in monocytes at a peak 30 min after stimulation. The presence of AGE-2 and AGE-3 did not influence the production of camp

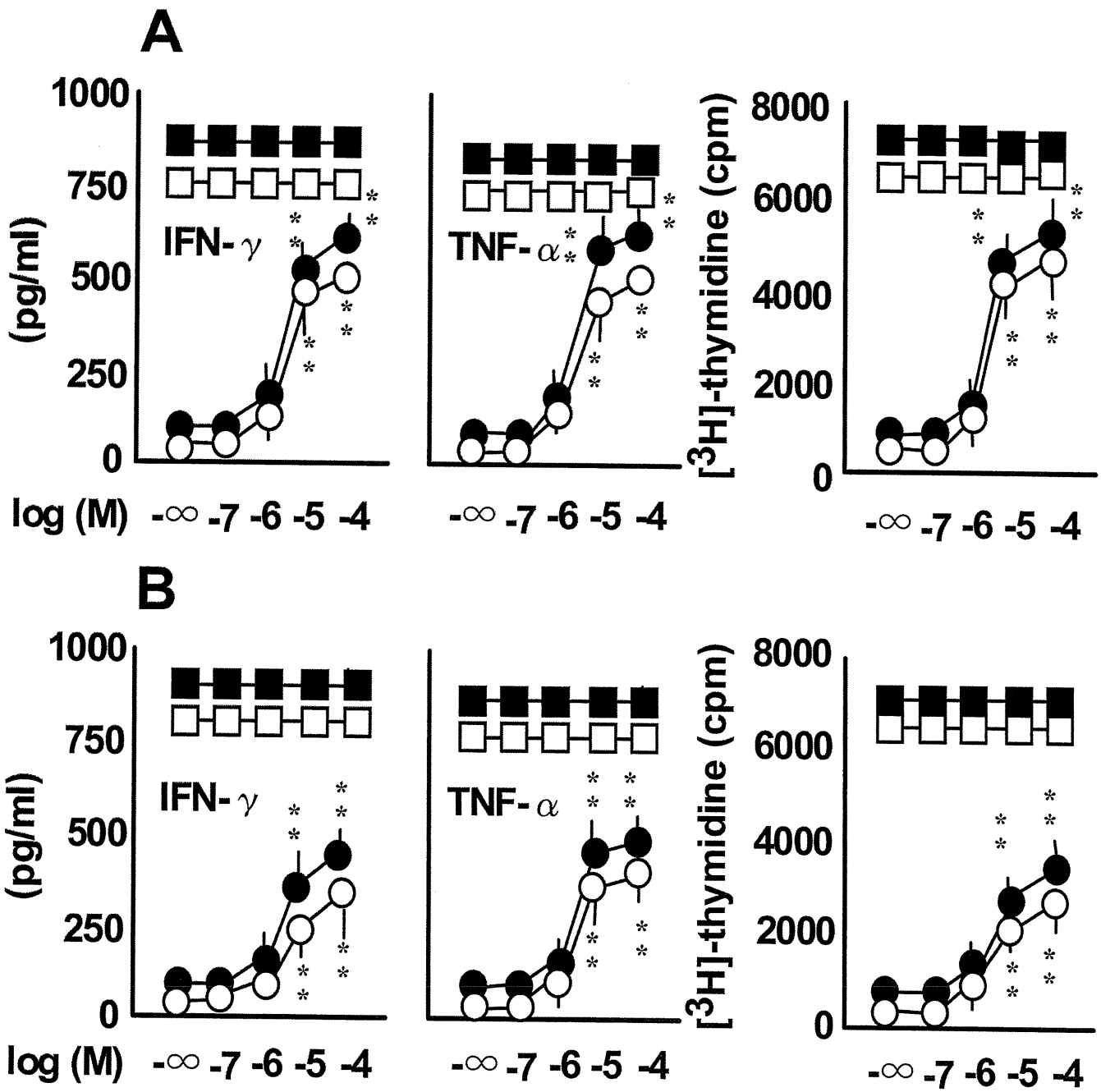

Fig. 7. The effects of prostanoid receptor antagonists on the inhibitory effect of PGE_2 on the production of IFN-γ and TNF-α and the lymphocyte proliferation PBMC at 1×10^6 cells/ml treated with PGE_2 at 1 μM were incubated with the EP_2 receptor antagonist, AH6809 (A), and the EP_4 receptor antagonist, AH23848 (B), at increasing concentrations from 0.1 to 100 μM in the presence of AGE-2 and AGE-3 at 100 μg/ml. IFN-γ and TNF-α concentrations in conditioned media were determined by ELISA. The lymphocyte proliferation was determined by [^{3}H]thymidine uptake as described under *Materials and Methods*. Filled circles (●) represent the effect of antagonists on PGE_2-inhibited adhesion molecule expression in the presence of AGE-2. Open circles (○) represent the effect of antagonists on PGE_2-inhibited adhesion molecule expression in the presence of AGE-3. Filled squares (■) represent the effect of antagonists on the actions of AGE-2 in the absence of PGE_2. Open squares (□) represent the effect of antagonists on the actions of AGE-3 in the absence of PGE_2. The results are expressed as the means ± S.E.M. of five donors with triplicate determinations. **, $P < 0.01$ compared with the values for PGE_2 in the presence of AGE-2 and AGE-3. When an error bar was within a symbol, the bar was omitted.

induced by PGE_2. EP_2 and EP_4 receptor agonists at 10 nM induced the production of camp (Fig. 8).

Involvement of cAMP in the Actions of PGE_2. To investigate the involvement of the cAMP/protein kinase A (PKA) pathway in the effects of PGE_2 on the expressions of ICAM-1, B7.1, B7.2, and CD40, the production of IFN-γ and TNF-α, and the lymphocyte proliferation, the effect of a PKA inhibitor, H89, at concentrations ranging from 0.1 to 100 μM, on the actions of PGE_2 in the presence of AGE-2 and AGE-3 at 100 μg/ml was determined (Figs. 9 and 10). H89 reversed the inhibitory effect of PGE_2 on AGE-2- and AGE-3-induced expressions of ICAM-1, B7.1, B7.2, and CD40, the production of IFN-γ and TNF-α, and the lymphocyte proliferation. On the other hand, H89 had no effect on the actions of AGE-2

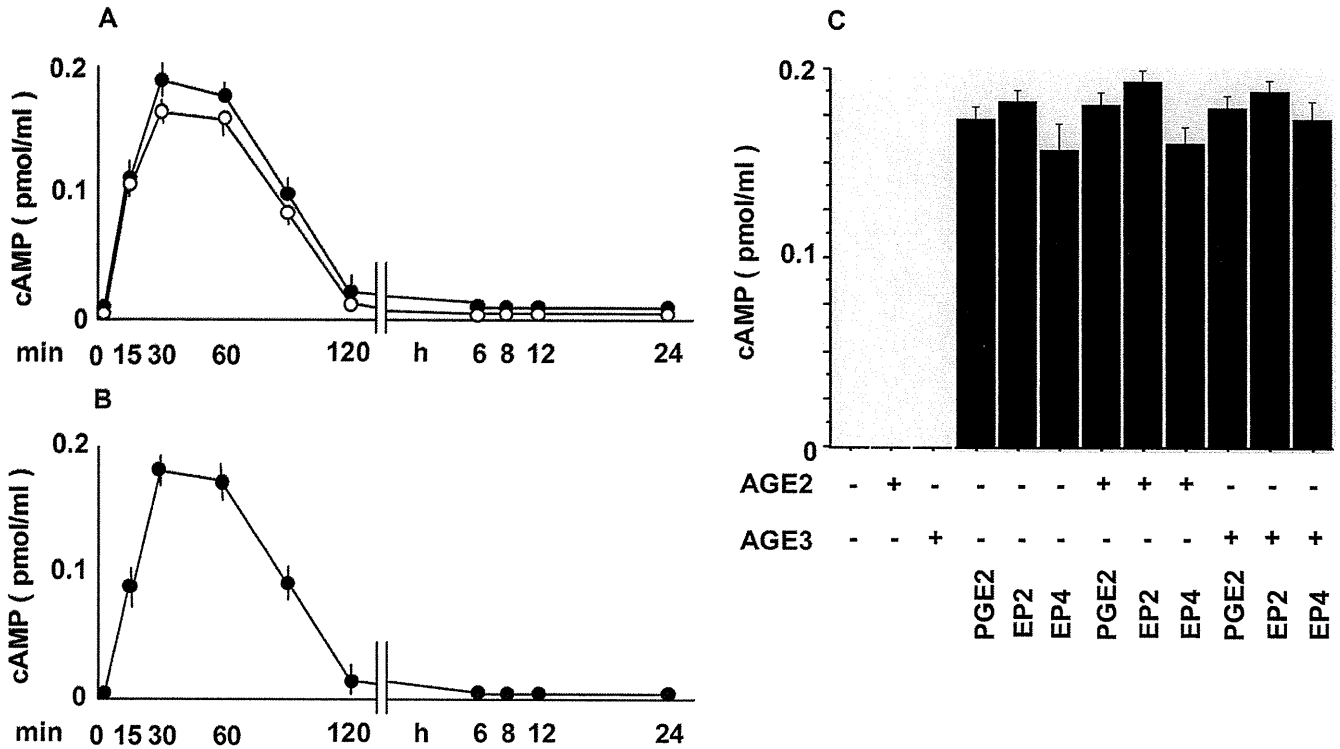

Fig. 8. The effects of PGE_2 on the production of cAMP in monocytes in the presence or absence of AGE-2 and AGE-3. A, monocytes at 1×10^6 cells/ml were incubated with PGE_2 at 10 nM in the presence (filled circles; ●) and absence (open circles; ○) of AGE-2 (A) and AGE-3 (B) at 100 μg/ml, and the time course changes in the levels of cAMP in monocytes were determined at the indicated time points. C, the effect of PGE_2, the EP_2 receptor agonist, ONO-AE1-259-01, and the EP^3 receptor agonist, ONO-AE-248, at 10 nM on the production of cAMP in the presence or absence of AGE-2 and AGE-3 at 30 min was determined. The results are expressed as the means ± S.E.M. of five donors with triplicate determinations. ND, not detected. When an error bar was within a symbol, the bar was omitted.

and AGE-3 in the absence of PGE_2. As shown in Figs. 11 and 12, the effects of a membrane-permeable cAMP analog, db-cAMP, and an adenylate cyclase activator, forskolin, at concentrations ranging from 0.1 to 100 μM, on the expressions of ICAM-1, B7.1, B7.2, and CD40 on monocytes, the production of IFN-γ and TNF-α, and the lymphocyte proliferation in PBMC in the presence of AGE-2 and AGE-3 at 100 μg/ml were examined. Both dbcAMP and forskolin inhibited AGE-2- and AGE-3-induced adhesion molecule expressions, the cytokine production, and the lymphocyte proliferation in a concentration-dependent manner.

Discussion

The level of glyceraldehyde-derived AGE (AGE-2) is reported to be 17 μg/ml in the serum of patient with diabetes (Enomoto et al., 2006; Nakamura et al., 2007). It is reported that AGEs at the concentrations ranging from 50 to 200 μg/ml remarkably induce human monocyte adhesion to bovine retinal endothelial cells (Mamputu et al., 2004). AGEs at 200 μg/ml induce the expression of CD40, CD80, and CD86 and the production of IFN-γ in dendritic cells (Ge et al., 2005). In the previous study, we found that AGE-2 and AGE-3 at 10 and 100 μg/ml significantly up-regulated the expressions of ICAM-1, B7.1, B7.2, and CD40, the production of IFN-γ and TNF-α, and the lymphocyte proliferation (Takahashi et al., 2009). Thus, the concentration used in the present study covers the pathological concentration of AGEs reported in the studies (Enomoto et al., 2006; Nakamura et al., 2007). Moreover, the accumulation of AGEs is shown in the atherosclerotic lesion by immunohistochemistry (Nakamura et al., 1993). It is probably that higher concentrations of AGEs may be present in the specific inflammatory lesions. Therefore, we determined the effects of AGEs at rather high pharmacological concentration (100 μg/ml).

In the present study, we found, for the first time, that PGE_2 inhibited AGE-2- and AGE-3-induced expressions of ICAM-1, B7.1, B7.2, and CD40, the production of IFN-γ and TNF-α, and the lymphocyte proliferation (Figs. 1 and 2). It is suggested that PGE_2 modulates inflammation during atherogenesis and other inflammatory diseases by suppressing macrophage-derived chemokine production via the EP_4 receptor (Takayama et al., 2002). To investigate receptor subtypes involved in the action of PGE_2, we used selective agonists for respective receptors (Suzawa et al., 2000). The EP_2 receptor agonist, ONO-AE1-259-01, and the EP_4 receptor agonist, ONO-AE1-329, were shown to be highly selective for mouse EP_2 and EP_4 receptors, respectively, using a receptor binding assay for Chinese hamster ovary cells transfected with each EP cDNA (Suzawa et al., 2000). It is reported that the selective EP_1, EP_2, EP_3, and EP_4 receptor agonists used in the present study were highly selective for their respective receptors (Suzawa et al., 2000). For example, the EP_2 receptor agonist, ONO-AE1-259, had at least 700-fold higher affinity for EP_2 receptors compared with other receptor agonists (Suzawa et al., 2000). As shown in Figs. 3 and 4, ONO-AE1-259 and ONO-AE-1-329 mimicked the effects of PGE_2 on the adhesion molecule expression, the cytokine pro-

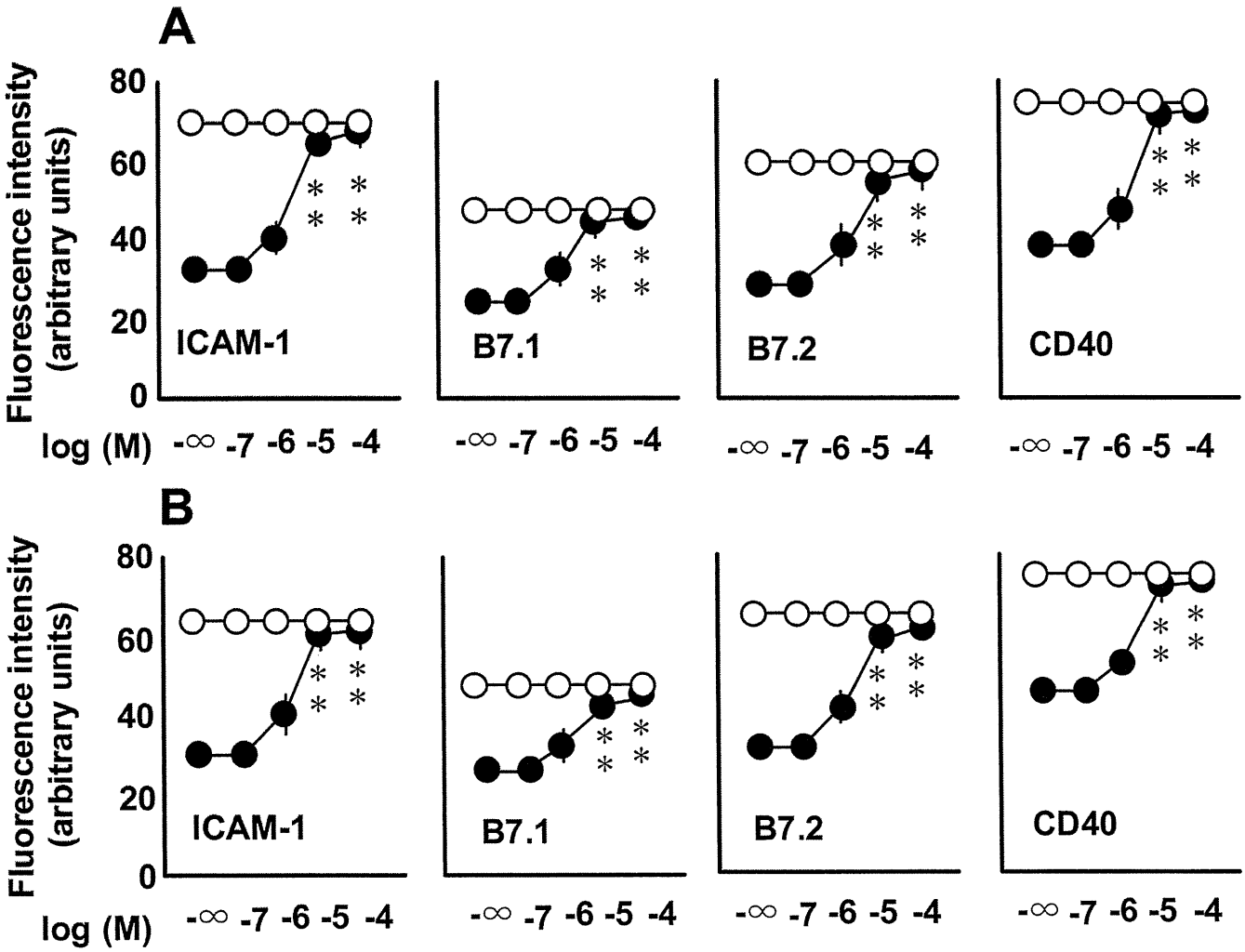

Fig. 9. The effects of PKA inhibitor on PGE_2-inhibited ICAM-1, B7.1, B7.2, and CD40 expressions. The effect of a PKA inhibitor, H89, at increasing concentrations from 0.1 to 100 μM on the expressions of ICAM-1, B7.1, B7.2, and CD40 on monocytes treated with PGE_2 at 10 nM in the presence of the AGE-2 (A) and AGE-3 (B) at 100 μg/ml was determined by flow cytometry. Filled circles (●) represent the effects of H89 on the PGE_2-induced inhibition of responses in the presence of AGE-2 and AGE-3. Open circles (○) represent the effects of H89 in the presence of AGE-2 and AGE-3 without PGE_2 stimulation. The results are expressed as the means ± S.E.M. of triplicate findings from five donors. **, $P < 0.01$ compared with the value for PGE_2. When an error bar was within a symbol, the bar was omitted.

duction, and the lymphocyte proliferation. In the present study, IC_{50} values for the inhibitory effects of ONO-AE1-259 and ONO-AE-1-329 on the expression of ICAM-1 on monocytes induced by AGE-2 and AGE-3 were similar, respectively (Table 1). It is unlikely that either receptor agonist stimulated the other receptors at the concentration range used judging from the selectivity of each agonist. As shown in Fig. 5, the observation that the mixed EP_2/EP_4 receptor agonist, 11-deoxy-PGE_1 (Noguchi et al., 2001), mimicked the inhibition of AGE-2- and AGE-3-induced adhesion molecule expression by PGE_2 was consistent with the above conclusion. Because the IC_{50} values of PGE_2 to prevent the upregulation of adhesion molecule expressions, cytokine production, and lymphocyte proliferation were consistent with the affinity of those agonists to typical EP_2 and EP_4 receptors (Table 1) (Takahashi et al., 2002). Moreover, the EP_2 receptor antagonist, AH6809, and the EP_4 receptor antagonist, AH23848, inhibited the actions of PGE_2 (Figs. 6 and 7). Therefore, it was suggested that the inhibitory effect of PGE_2 was mediated by the stimulation of EP_2 and EP_4 receptors but not EP_1 and EP_3 receptors.

It is known that the stimulation of EP_2 and EP_4 receptors induces the production of cAMP (Coleman et al., 1994). As shown in Fig. 8, PGE_2, EP_2, and EP_4 receptor agonists induced the production of cAMP in monocytes irrespective of the presence of AGE-2 and AGE-3. The PKA inhibitor, H89, inhibited the action of PGE_2 (Figs. 9 and 10), and the cAMP analog, dbcAMP, and the adenylate cyclase activator, forskolin, mimicked the effect of PGE_2 (Figs. 11 and 12). These results suggested the involvement of the EP_2/EP_4 receptor-cAMP/PKA pathway in the actions of PGE_2. In addition, the present data were consistent with the finding that the elevation of cAMP prevents the production of TNF-α in monocytes of diabetic patients (Jain et al., 2002). We observed a similar pattern of the inhibitory effects of PGE_2 on IL-18-induced activation of monocytes in human PBMC via EP_2 and EP_4 receptors (Takahashi et al., 2002). Thus, there may be a common pathway triggered by IL-18 and AGEs that was

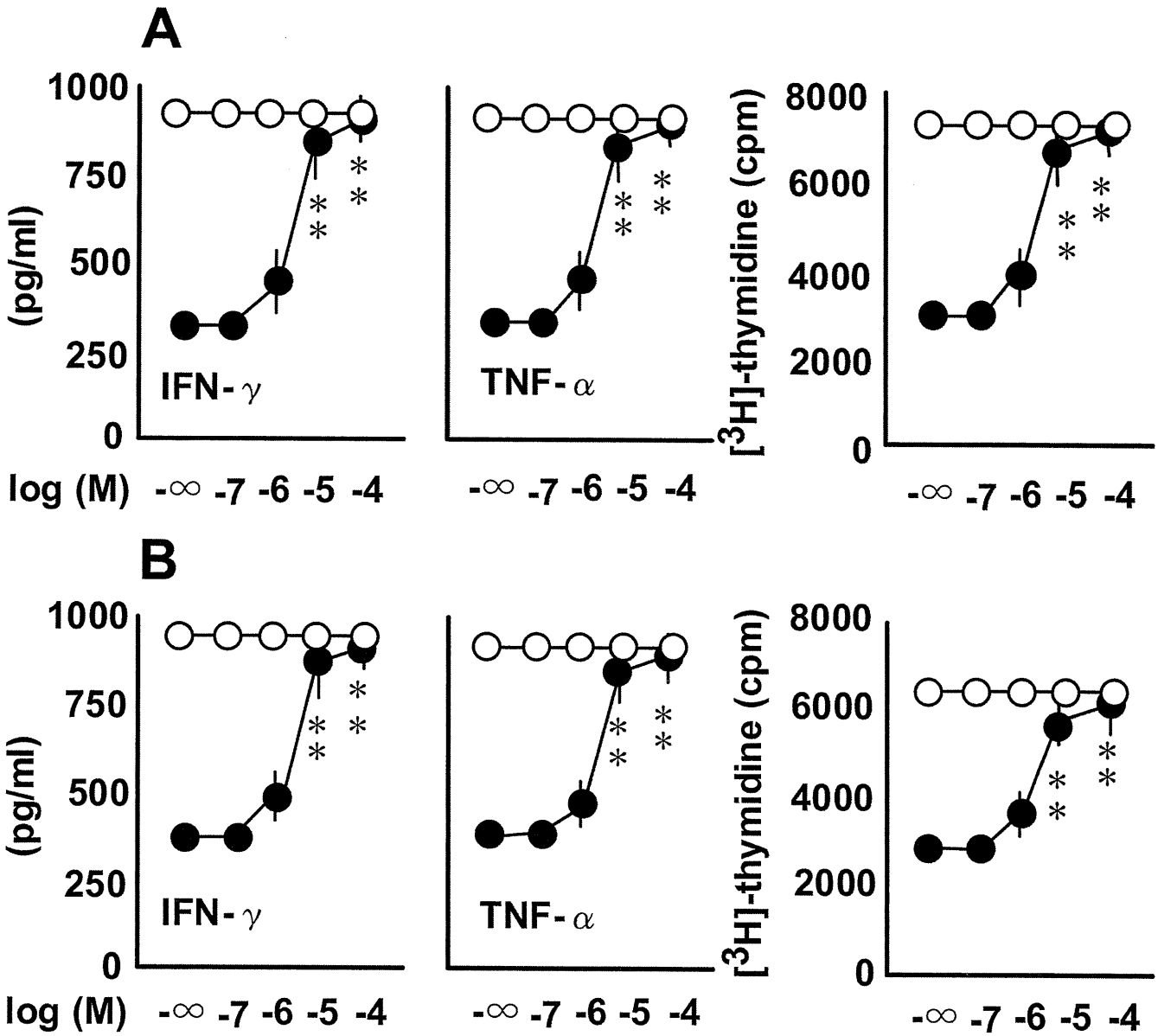

Fig. 10. The effects of PKA inhibitor on PGE_2-inhibited TNF-α and IFN-γ production and the lymphocyte proliferation. The effect of a PKA inhibitor, H89, at increasing concentrations from 0.1 to 100 μM on the production of TNF-α and IFN-γ in PBMC treated with PGE_2 at 10 nM in the presence of AGE-2 (A) and AGE-3 (B) at 100 μg/ml was determined by ELISA. The lymphocyte proliferation was determined by [^{3}H]thymidine uptake as described under *Materials and Methods*. Filled circles (●) represent the effects of H89 on the PGE_2-induced inhibition of responses in the presence of AGE-2 and AGE-3. Open circles (○) represent the effects of H89 in the presence of AGE-2 and AGE-3 without PGE_2 stimulation. The results are expressed as the means ± S.E.M. of triplicate findings from five donors. **, $P < 0.01$ compared with the value for PGE_2. When an error bar was within a symbol, the bar was omitted.

regulated by the EP_2/EP_4 receptor-cAMP/PKA system. Further work is necessary on this issue.

In the previous study, we found that AGE-2 and AGE-3 had higher affinity for RAGE than AGE-4 and AGE-5 using an in vitro binding assay (Takahashi et al., 2009). AGE-2 and AGE-3, but not AGE-4 and AGE-5, induced the up-regulation of their receptor RAGE expression on the cell surface of monocytes. PGE_2 had no effect on the expression of RAGE in the presence and absence of AGE-2 and AGE-3 (data not shown), suggesting that there might be distinct signal transduction pathways of RAGE activation, leading to enhanced expression of adhesion molecule and RAGE, which were differentially regulated by the cAMP/PKA system.

RAGE is predominantly localized with lesional macrophages in human carotid atherosclerotic plaques, where macrophages also represent the majority of COX-2-expressing cells (Cuccurullo et al., 2006). It is reported that AGEs ligate cell-surface RAGE on the vascular endothelium, mononuclear phagocytes, vascular smooth muscle, and neurons to activate cell signaling pathways such as P44/P42 mitogen-activated protein kinase and NF-κB (Yan et al., 1994; Lander et al., 1997), redirecting cellular function in a manner linked to the expression of inflammatory and prothrombotic genes important in the pathogenesis of chronic disorders such as diabetic microvascular disease and amyloidosis (Schmidt et al., 1994; Miyata et al., 1996; Park et al., 1998). When stim-

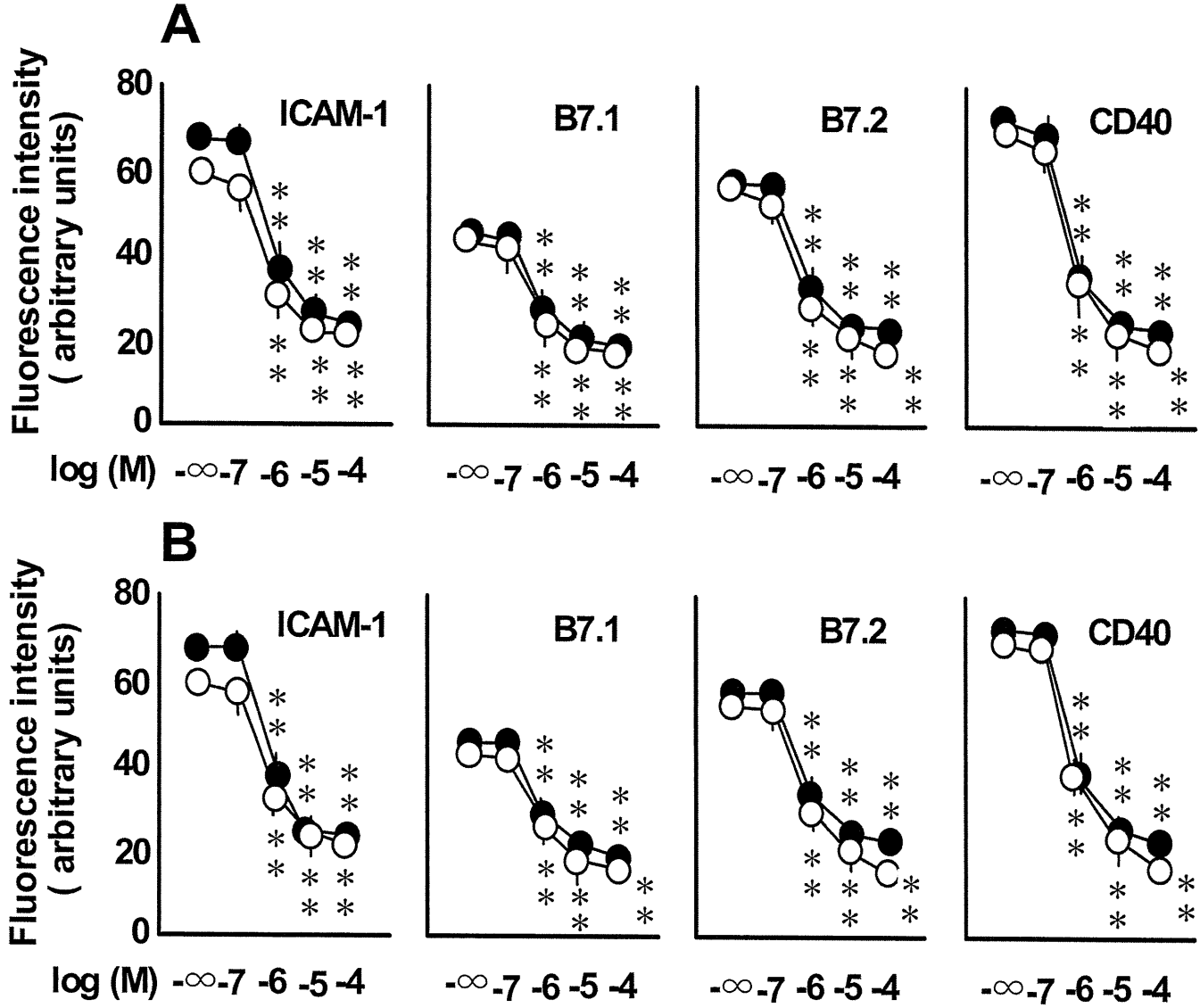

Fig. 11. The effects of forskolin and dbcAMP on AGE-induced ICAM-1, B7.1, B7.2, and CD40 expressions on human monocytes. PBMC at 1×10^6/ml were incubated with an adenylate cyclase activator, forskolin (A), and a cAMP analog, dbcAMP (B), at increasing concentrations from 0.1 to 100 μM in the presence of AGE-2 (filled circles; ●) and AGE-3 (open circles; ○) at 100 μg/ml for 24 h. The expressions of ICAM-1, B7.1, B7.2, and CD40 on monocytes were determined by flow cytometry. The results are expressed as the means ± S.E.M. of five donors with triplicate determinations. **, $P < 0.01$ compared with the values for AGE-2 and AGE-3. When an error bar was within a symbol, the bar was omitted.

ulated with lipopolysaccharide, zymosan, or polymerized bovine albumin (Penglis et al., 2000), the expression of COX-2 was specifically up-regulated, leading to enhanced production of PGE_2. Lipopolysaccharide-treated monocytes/macrophages activate multiple signal transduction pathways, including the activation of NF-κB and c-Jun NH_2-terminal kinase. Some of these pathways, in part, may be shared by RAGE signaling. However, we confirmed that AGE-2, AGE-3, AGE-4, and AGE-5 at 100 μg/ml had no effect on the expression of COX-2 mRNA and protein in human monocytes (data not shown). In the present study, we examined the effect of a nonselective COX-2 inhibitor, indomethacin, and a selective COX-2 inhibitor, NS-398, on the actions of PGE_2 in the presence or absence of AGE-2 and AGE-3. The COX-2 inhibitors had no effect on the expressions of adhesion molecule, the cytokine production, and the lymphocyte proliferation (data not shown). In addition, AGE-2, AGE-3, AGE-4, and AGE-5 had no effect on PGE_2 production (data not shown). Therefore, it is probably that the endogenous production of PGE_2 in monocytes did not occur under the present conditions.

It is reported that PGE_2 induced by monocytes inhibits procollagen secretion by human vascular smooth muscle cells, leading to extracellular matrix remodeling and resistance to rupture during atherosclerosis (Fitzsimmons et al., 1999). Elevation of cAMP in endothelial cells inhibits proliferation, leading to the inhibition of atherosclerosis in patients with diabetes (Lorenowicz et al., 2007). Together with these results and our data, other extracellular stimuli, which induce intracellular cAMP production on binding to their cognate G protein-coupled receptors, may regulate the activation of vascular smooth muscle cells and endothelial cells. In conclusion, PGE_2 inhibited AGE-2-

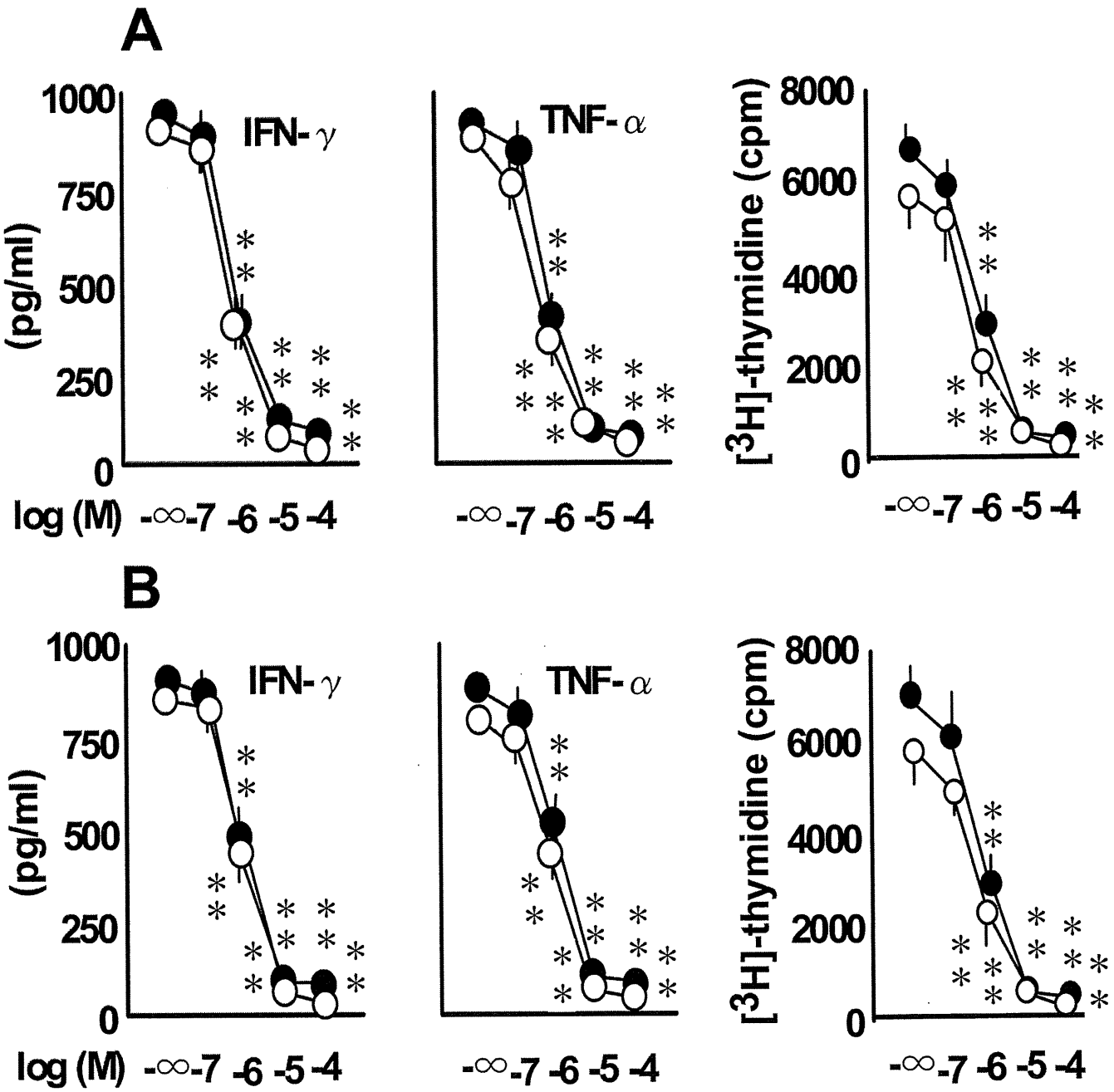

Fig. 12. The effects of forskolin and dbcAMP on AGE-induced IFN-γ and TNF-α production and the lymphocyte proliferation in PBMC. PBMCs at 1×10^6/ml were incubated with an adenylate cyclase activator, forskolin (A), and a cAMP analog, dbcAMP (B), at increasing concentrations from 0.1 to 100 μM in the presence of AGE-2 (filled circles; ●) and AGE-3 (open circles; ○) at 100 μg/ml for 24 h. IFN-γ and TNF-α concentrations in conditioned media were determined by ELISA. The lymphocyte proliferation was determined by [^{3}H]thymidine uptake as described under *Materials and Methods*. The results are expressed as the means ± S.E.M. of five donors with triplicate determinations. **, $P < 0.01$ compared with the values for AGE-2 and AGE-3. When an error bar was within a symbol, the bar was omitted.

and AGE-3-induced expressions of ICAM-1, B7.1, B7.2, and CD40, the production of IFN-γ and TNF-α, and the lymphocyte proliferation via EP_2/EP_4 receptors and the cAMP/PKA pathway. Through the inhibition of toxic AGE-dependent responses in monocytes, the stimulation of EP_2 and EP_4 receptors may partially contribute to regulation of the development of atherosclerotic plaques in diabetes. The present study might lead to an exploration of the therapeutic potential of PGE_2 on the systemic inflammatory response evoked by diabetes.

Acknowledgments

We thank Ono Pharmaceutical Co. (Tokyo, Japan) for donating ONO-D1-004, ONO-AE1-259-01, ONO-AE-248, ONO-AE1-329, and 11-deoxy-PGE_1. We also thank Miyuki Shiotani and Yukinari Isomoto for technical assistance.

References

Bierhaus A, Hofmann MA, Ziegler R, and Nawroth PP (1998) AGEs and their interaction with AGE-receptors in vascular disease and diabetes mellitus. I. The AGE concept. *Cardiovasc Res* **37:**586–600.

Bierhaus A, Illmer T, Kasper M, Luther T, Quehenberger P, Tritschler H, Wahl P, Ziegler R, Müller M, and Nawroth PP (1997) Advanced glycation end product (AGE)-mediated induction of tissue factor in cultured endothelial cells is dependent on RAGE. *Circulation* **96:**2262–2271.

Brownlee M, Cerami A, and Vlassara H (1988) Advanced glycosylation end products in tissue and the biochemical basis of diabetic complications. *N Engl J Med* **318:**1315–1321.

Burke AP, Kolodgie FD, Zieske A, Fowler DR, Weber DK, Varghese PJ, Farb A, and Virmani R (2004) Morphologic findings of coronary atherosclerotic plaques in diabetics: a postmortem study. *Arterioscler Thromb Vasc Biol* **24:**1266–1271.

Camacho SA, Heath WR, Carbone FR, Sarvetnick N, LeBon A, Karlsson L, Peterson PA, and Webb SR (2001) A key role for ICAM-1 in generating effector cells mediating inflammatory responses. *Nat Immunol* **6:**523–529.

Coleman RA, Smith WL, and Narumiya S (1994) VIII. International Union of Pharmacology classification of prostanoid receptors: properties, distribution, and structure of the receptor and their subtypes. *Pharmacol Rev* **46:**205–229.

Cuccurullo C, Iezzi A, Fazia ML, De Cesare D, Di Francesco A, Muraro R, Bei R, Ucchino S, Spigonardo F, Chiarelli F, et al. (2006) Suppression of RAGE as a basis of simvastatin-dependent plaque stabilization in type 2 diabetes. *Arterioscler Thromb Vasc Biol* **26:**2716–2723.

Durie FH, Foy TM, Masters SR, Laman JD, and Noelle RJ (1994) The role of CD40 in the regulation of humoral and cell-mediated immunity. *Immunol Today* **9:**406–411.

Enomoto M, Adachi H, Yamagishi S, Takeuchi M, Furuki K, Hino A, Hiratsuka A, Takajo Y, and Imaizumi T (2006) Positive association of serum levels of advanced glycation end products with thrombogenic markers in humans. *Metabolism* **55:**912–917.

Fitzsimmons C, Proudfoot D, and Bowyer DE (1999) Monocyte prostaglandins inhibit procollagen secretion by human vascular smooth muscle cells: implications for plaque stability. *Atherosclerosis* **142:**287–293.

Fukami K, Ueda S, Yamagishi S, Kato S, Inagaki Y, Takeuchi M, Motomiya Y, Bucala R, Iida S, Tamaki K, et al. (2004) AGEs activate mesangial TGF-beta-Smad signaling via an angiotensin II type I receptor interaction. *Kidney Int* **66:**2137–2147.

Ge J, Jia Q, Liang C, Luo Y, Huang D, Sun A, Wang K, Zou Y, and Chen H (2005) Advanced glycosylation end products might promote atherosclerosis through inducing the immune maturation of dendritic cells. *Arterioscler Thromb Vasc Biol* **25:**2157–2163.

Hempel SL, Monick MM, and Hunninghake GW (1994) Lipopolysaccharide induces prostaglandin H synthase-2 protein and mRNA in human alveolar macrophages and blood monocytes. *J Clin Invest* **93:**391–396.

Hofmann MA, Drury S, Fu C, Qu W, Taguchi A, Lu Y, Avila C, Kambham N, Bierhaus A, Nawroth P, et al. (1999) RAGE mediates a novel proinflammatory axis: a central cell surface receptor for S100/calgranulin polypeptides. *Cell* **97:**889–901.

Jain SK, Kannan K, Lim G, McVie R, and Bocchini JA Jr (2002) Hyperketonemia increases tumor necrosis factor-α secretion in cultured U937 monocytes and type 1 diabetic patients and is apparently mediated by oxidative stress and cAMP deficiency. *Diabetes* **51:**2287–2293.

Kay LJ, Yeo WW, and Peachell PT (2006) Prostaglandin E2 activates EP2 receptors to inhibit human lung mast cell degranulation. *Br J Pharmacol* **147:**707–713.

Lander HM, Tauras JM, Ogiste JS, Hori O, Moss RA, and Schmidt AM (1997) Activation of the receptor for advanced glycation end products triggers a p21(ras)-dependent mitogen-activated protein kinase pathway regulated by oxidant stress. *J Biol Chem* **272:**17810–17814.

Lorenowicz MJ, Fernandez-Borja M, and Hordijk PL (2007) cAMP signaling in leukocyte transendothelial migration. *Arterioscler Thromb Vasc Biol* **27:**1014–1022.

Mamputu JN and Renier (2004) Advanced glycation end-products increase monocyte adhesion to retinal endothelial cells through vascular endothelial growth factor-induced ICAM-1 expression: inhibitory effect of antioxidants. *J Leukocyte Biol* **75:**1062–1069.

Miyata T, Hori O, Zhang J, Yan SD, Ferran L, Iida Y, and Schmidt AM (1996) The receptor for advanced glycation end products (RAGE) is a central mediator of the interaction of AGE-beta2microglobulin with human mononuclear phagocytes via an oxidant-sensitive pathway. Implications for the pathogenesis of dialysis-related amyloidosis. *J Clin Invest* **98:**1088–1094.

Nakamura K, Yamagishi SI, Matsui T, Adachi H, Takeuchi M, and Imaizumi T (2007) Serum levels of soluble form of receptor for advanced glycation end products (sRAGE) are correlated with AGEs in both diabetic and non-diabetic subjects. *Clin Exp Med* **7:**188–190.

Nakamura Y, Horii Y, Nishino T, Shiiki H, Sakaguchi Y, Kagoshima T, Dohi K, Makita Z, Vlassara H, and Bucala R (1993) Immunohistochemical localization of advanced glycosylation end products in coronary atheroma and cardiac tissue in diabetes mellitus. *Am J Pathol* **143:**1649–1656.

Noguchi K, Iwasaki K, Shitashige M, Umeda M, Izumi Y, Murota S, and Ishikawa I (2001) Downregulation of lipopolysaccharide-induced intercellular adhesion molecule-1 expression via EP2/EP4 receptors by prostaglandin E2 in human fibroblasts. *Inflammation* **25:**75–81.

Okamoto T, Yamagishi S, Inagaki Y, Amano S, Koga K, Abe R, Takeuchi M, Ohno S, Yoshimura A, and Makita Z (2002) Angiogenesis induced by advanced glycation end products and its prevention by cerivastatin. *FASEB J* **16:**1928–1930.

Park L, Raman KG, Lee KJ, Lu Y, Ferran LJ Jr, Chow WS, Stern D, and Schmidt AM (1998) Suppression of accelerated diabetic atherosclerosis by the soluble receptor for advanced glycation endproducts. *Nat Med* **4:**1025–1031.

Penglis PS, Cleland LG, Demasi M, Caughey GE, and James MJ (2000) Differential regulation of prostaglandin E2 and thromboxane A2 production in human monocytes: implications for the use of cyclooxygenase inhibitors. *J Immunol* **165:**1605–1611.

Ranger AM, Das MP, Kuchroo VK, and Glimcher LH (1996) B7-2 (CD86) is essential for the development of IL-4-producing T cells. *Int Immunol* **8:**1549–1560.

Schmidt AM, Hasu M, Popov D, Zhang JH, Chen J, Yan SD, Brett J, Cao R, Kuwabara K, and Costache G (1994) Receptor for advanced glycation end products (AGEs) has a central role in vessel wall interactions and gene activation in response to circulating AGE proteins. *Proc Natl Acad Sci U S A* **91:**8807–8811.

Schmidt AM, Hori O, Chen JX, Li JF, Crandall J, Zhang J, Cao R, Yan SD, Brett J, and Stern D (1995) Advanced glycation endproducts interacting with their endothelial receptor induce expression of vascular cell adhesion molecule-1 (VCAM-1) in cultured human endothelial cells and in mice. A potential mechanism for the accelerated vasculopathy of diabetes. *J Clin Invest* **96:**1395–1403.

Stoll G and Bendszus M (2006) Inflammation and atherosclerosis: novel insights into plaque formation and destabilization. *Stroke* **37:**1923–1932.

Suzawa T, Miyaura C, Inada M, Maruyama T, Sugimoto Y, Ushikubi F, Ichikawa A, Narumiya S, and Suda T (2000) The role of prostaglandin E receptor subtypes (EP1, EP2, EP3, and EP4) in bone resorption: an analysis using specific agonists for the respective EPs. *Endocrinology* **141:**1554–1559.

Takahashi HK, Iwagaki H, Tamura R, Xue D, Sano M, Mori S, Yoshino T, Tanaka N, and Nishibori M (2003) Unique regulation profile of prostaglandin E1 on adhesion molecule expression and cytokine production in human peripheral blood mononuclear cells. *J Pharmacol Exp Ther* **307:**1188–1195.

Takahashi HK, Iwagaki H, Yoshino T, Mori S, Morichika T, Itoh H, Yokoyama M, Kubo S, Kondo E, Akagi T, et al. (2002) Prostaglandin E(2) inhibits IL-18-induced ICAM-1 and B7.2 expression through EP2/EP4 receptors in human peripheral blood mononuclear cells. *J Immunol* **168:**4446–4454.

Takahashi HK, Mori S, Wake H, Liu K, Yoshino T, Ohashi K, Tanaka N, Shikata K, Makino H, and Nishibori M (2009) Advanced glycation end products subspecies-selectively induce adhesion molecule expression and cytokine production in human peripheral blood mononuclear cells. *J Pharmacol Exp Ther* **330:**89–98.

Takayama K, García-Cardena G, Sukhova GK, Comander J, Gimbrone MA Jr, and Libby P (2002) Prostaglandin E2 suppresses chemokine production in human macrophages through the EP4 receptor. *J Biol Chem* **277:**44147–44154.

Takeuchi M, Makita Z, Bucala R, Suzuki T, Koike T, and Kameda Y (2000) Immunological evidence that non-carboxymethyllysine advanced glycation end-products are produced from short chain sugars and dicarbonyl compounds in vivo. *Mol Med* **6:**114–125.

Takeuchi M and Yamagishi S (2004) TAGE (toxic AGEs) hypothesis in various chronic diseases. *Medical Hypotheses* **63:**449–452.

Wake H, Takahashi HK, Mori S, Liu K, Yoshino T, and Nishibori M (2009) Histamine inhibits advanced glycation end products-induced adhesion molecule expression on human monocytes. *J Pharmacol Exp Ther* **330:**826–833.

Wautier JL, Zoukourian C, Chappey O, Wautier MP, Guillausseau PJ, Cao R, Hori O, Stern D, and Schmidt AM (1996) Receptor-mediated endothelial cell dysfunction in diabetic vasculopathy. Soluble receptor for advanced glycation end products blocks hyperpermeability in diabetic rats. *J Clin Invest* **97:**238–243.

Yamagishi S, Amano S, Inagaki Y, Okamoto T, Koga K, Sasaki N, Yamamoto H, Takeuchi M, and Makita Z (2002) Advanced glycation end products-induced apoptosis and overexpression of vascular endothelial growth factor in bovine retinal pericytes. *Biochem Biophys Res Commun* **290:**973–978.

Yan SD, Schmidt AM, Anderson GM, Zhang J, Brett J, Zou YS, Pinsky D, and Stern D (1994) Enhanced cellular oxidant stress by the interaction of advanced glycation end products with their receptors/binding proteins. *J Biol Chem* **269:**9889–9897.

Address correspondence to: Masahiro Nishibori, Department of Pharmacology, Okayama University Graduate School of Medicine and Dentistry, 2-5-1 Shikata-cho, Okayama 700-8558, Japan. E-mail: mbori@md.okayama-u.ac.jp

Acta Med. Okayama, 2009
Vol. 63, No. 5, pp. 249-262

Acta Medica Okayama
http://escholarship.lib.okayama-u.ac.jp/amo/

Original Article

High Mobility Group Box 1 Complexed with Heparin Induced Angiogenesis in a Matrigel Plug Assay

Hidenori Wake[a], Shuji Mori[b], Keyue Liu[a],
Hideo K. Takahashi[a], and Masahiro Nishibori[a]*

[a]*Department of Pharmacology, Okayama University Graduate School of Medicine, Dentistry and Pharmaceutical Sciences, Okayama 700-8558, Japan, and*
[b]*Shujitsu University, School of Pharmacy, Okayama 703-8516, Japan*

Angiogenesis involves complex processes mediated by several factors and is associated with inflammation and wound healing. High mobility group box 1 (HMGB1) is released from necrotic cells as well as macrophages and plays proinflammatory roles. In the present study, we examined whether HMGB1 would exhibit angiogenic activity in a matrigel plug assay in mice. HMGB1 in combination with heparin strongly induced angiogenesis, whereas neither HMGB1 nor heparin alone showed such angiogenic activity. The heparin-dependent induction of angiogenesis by HMGB1 was accompanied by increases in the expression of tumor necrosis factor-α (TNF-α) and vascular endothelial growth factor-A_{120} (VEGF-A_{120}). It is likely that the dependence of the angiogenic activity of HMGB1 on heparin was due to the efficiency of the diffusion of the HMGB1-heparin complex from matrigel to the surrounding areas. VEGF-A_{165} possessing a heparin-binding domain showed a pattern of heparin-dependent angiogenic activity similar to that of HMGB1. The presence of heparin also inhibited the degradation of HMGB1 by plasmin *in vitro*. Taken together, these results suggested that HMGB1 in complex with heparin possesses remarkable angiogenic activity, probably through the induction of TNF-α and VEGF-A_{120}.

Key words: angiogenesis, HMGB1, heparin

Angiogenesis is an essential process by which new blood vessels are formed and accompanies embryonic development, inflammation and wound healing. Angiogenesis may also be involved in several disease conditions, including cancers, rheumatic arthritis, diabetic retinopathy and atherosclerosis. The process of angiogenesis appears to be under the control of a complex system consisting of proangiogenic and antiangiogenic factors. From the cellular perspective, angiogenesis is a series of processes that induce the proliferation and migration of vascular endothelial cells (ECs), in association with the activation of macrophages. These cells together with stromal cells produce active substances such as matrix metalloproteinases (MMPs), a variety of cytokines and growth factors [1-3].

High mobility group box 1 (HMGB1), a non-histone nuclear protein involved in maintaining the architectural structure of DNA and the regulation of transcription, is secreted from necrotic cells and activated macrophages. Once released into the extracellular space, HMGB1 acts as a cytokine [4-8]. HMGB1 is

Received March 26, 2009; accepted May 26, 2009.
*Corresponding author. Phone:+81-86-235-7140; Fax:+81-86-235-7140
E-mail:mbori@md.okayama-u.ac.jp (M. Nishibori)

widely distributed in all types of cells and is highly conserved throughout species [9]. HMGB1 has a unique structure consisting of 3 domains. The A-box and B-box domains are rich in basic amino acids and bind to DNA, while the C-terminal domain is composed of acidic amino acid clusters [10]. It has been suggested that amino acids 6–12 bind to heparin, and that amino acids 150–183 bind to the receptor for advanced glycation end products (RAGE) [11, 12]. The expression of HMGB1 is increased in inflammatory conditions such as sepsis [13], atherosclerosis [14] and rheumatic arthritis [15]. HMGB1 is also secreted from several tumor cells [16–20]. Secreted HMGB1 may bind to RAGE, toll-like receptor 2 (TLR2) and toll-like receptor 4 (TLR4) expressed on the surfaces of monocytes/macrohpages, and such bindings activate NF-κB [21–23], thereby facilitating the inflammatory response through the expression and secretion of inflammatory cytokines (tumor necrosis factor-α (TNF-α), IL-1α, IL-1β, IL-6, IL-8, *etc.*) [24]. In addition, HMGB1 may be closely related to angiogenesis during inflammation, since recent studies revealed that HMGB1 induces sprouting and chemotaxis of ECs and promotes angiogenesis in the chick embryo chorioallantoic membrane [25, 26]. However, there have been few studies on the effects of HMGB1 on angiogenesis in *in vivo* mammalian models.

In this study, we examined the effect of HMGB1 on angiogenesis *in vivo* using a matrigel system and demonstrated that HMGB1 induced angiogenesis in a heparin-dependent manner. This angiogenesis may occur through the expression of TNF-α and vascular endothelial growth factor-A_{120} (VEGF-A_{120}) in the surrounding areas of the matrigel.

Materials and Methods

Reagents. Matrigel is a mixture of basement membrane components extracted from Engelbreth-Holm-Swarm (EHS) tumors inoculated in C57BL/6J mice. The matrigel was prepared as previously described [27], and was not supplemented with any growth factors. Matrigel mainly contains laminin, collagen IV, heparan sulfate proteoglycan and entactin. Since matrigel is a liquid at 4℃ and turns into a gel at 22–35℃, we injected ice-cold matrigel solution into the backs of mice to allow the gel to form subcutaneously, as shown in Fig. 1. Anti-rat IgG goat polyclonal IgG-HRP was obtained from Santa Cruz Biotechnology (Santa Cruz, CA, USA). Rat monoclonal anti-bovine HMGB1 antibody (#10–22) was produced as described previously [28].

Animals. Male C57BL/6J mice (24–26 g, 7–8 wk) were obtained from the Department of Animal Resources of Okayama University. All animal experiments were performed according to the guidelines of Okayama University on animal experiments, were approved by the University's committee on animal experimentation and conformed to the Guide for the Care and Use of Laboratory Animals published by the US National Institutes of Health (NIH Publication No. 85–23, revised 1996). Mice were housed with a 12-h light-dark cycle at 22℃ with water and food ad libitum.

Methods.

1. Expression and purification of HMGB1.

Full-length human HMGB1 DNA was amplified by PCR using Cap Site cDNA dT from human microvascular endothelial cells (Nippon Gene, Tokyo, Japan) and primers (forward 5'-GCA GAA TTC ATG GGC AAA GGA GAT CCT A-3', reverse 5'-CAT CTC GAG TCA TTA TTC ATC ATC ATC ATC-3'). The full-length HMGB1 DNA fragment and pGEX-6p-1 vector (GE Healthcare, Little Chalfont, England) were digested with EcoRI and XhoI (New England Biolabs, Ipswich, UK) restriction enzymes. The DNA fragment was subcloned into the vector. The recombinant plasmids were transformed into *E. coli* strain BL21 (DE3) (Merck, San Diego, CA, USA). The transformants were incubated overnight at 37℃ to express the recombinant GST-HMGB1 in Overnight Express Instant TB medium (Merck). *E. coli* extract containing GST-HMGB1 fusion proteins was applied to glutathione-Sepharose 4B and incubated for 1 h at room temperature. After extensive washing, the gel bed was incubated with PreScission Protease for 3 h at 4℃. After brief centrifugation, the supernatant containing GST-tag-deleted HMGB1 was collected and purified by gel filtration chromatography using TSK-gel 3000SW_{XL} (Tosoh, Tokyo, Japan) [29]. Purified recombinant human HMGB1 protein was identified by SDS-PAGE [30] and Western blotting [31] with anti-HMGB1 monoclonal antibody (#10–22). The final HMGB1 preparation contained lipopolysaccharide (LPS) of less than 2.0 pg/μg protein.

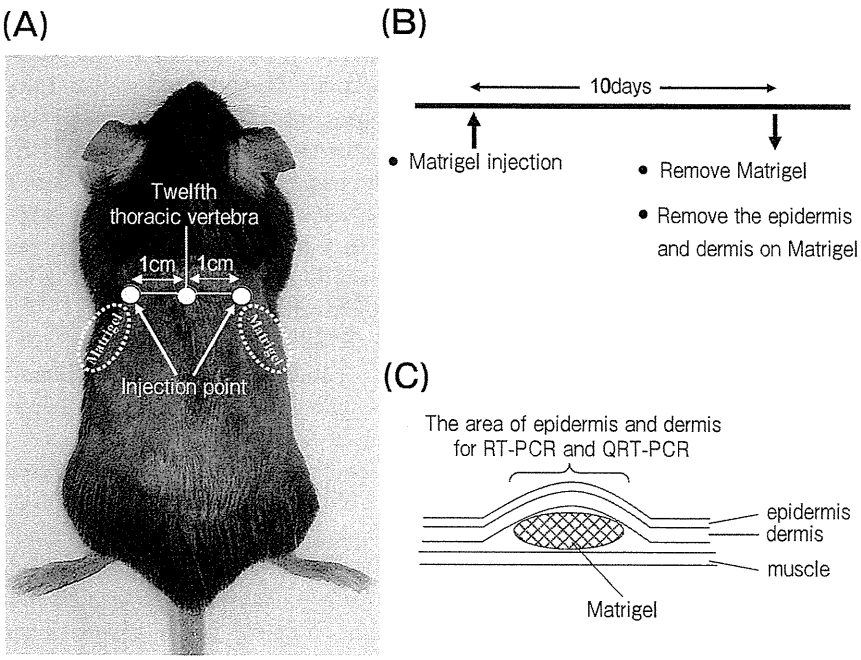

Fig. 1 *In vivo* matrigel angiogenesis plug assay method. (A) The injection point of matrigel into the mouse back is indicated. For the PBS control, matrigel was inoculated on the left side and for the other groups, it was inoculated on the right side. (B) The protocols of matrigel injection and sampling are shown. (C) The sampling area of mouse skin for RT-PCR or real-time PCR is shown.

2. *In vivo* matrigel plug assay.

At 4℃, 500μl of matrigel solution (8.4mg protein/ml) was mixed with PBS, HMGB1 (2.5μg/ml, 100nM), heparin (320μg/ml, 64units/ml) (Sigma, St. Louis, MO, USA), heparin+HMGB1, human VEGF-A_{121} (185ng/ml, 6.5nM or 1.85μg/ml, 65nM) (Peprotech, Rocky Hill, CT, USA), human VEGF-A_{165} (250ng/ml, 6.5nM) (Peprotech), human VEGF-A_{121}+heparin, or human VEGF-A_{165}+heparin. Male C57BL/6J mice were anesthetized with 50% N_2O+50% O_2 and the liquid matrigel mixture was injected subcutaneously into the back using a 25G needle. The liquid matrigel mixture was solidified 5–10min after injection (Fig. 1A). Mice were sacrificed at the indicated time points by cervical dislocation and the matrigel plugs were recovered for analysis of angiogenesis (Fig. 1B).

3. Quantification of hemoglobin in matrigel.

The removed matrigel plugs were homogenized in 10mM PBS (pH7.4) and centrifuged at 8,000×g for 10min. The hemoglobin contents in the supernatant were determined using a Hemoglobin B test kit (Wako, Osaka, Japan) according to the manufacturer's instructions.

4. Immunohistochemistry.

Matrigel plugs were fixed with 10% formalin-0.1 M phosphate buffer and embedded in paraffin for HE and immunohistochemical stainings. Immunohistochemical staining of CD31 was performed on 5μm matrigel sections with rabbit polyclonal anti-mouse CD31 antibody (Abcam, Cambridge, UK) followed by a secondary antibody, anti-rabbit IgG goat IgG-HRP (Abcam). Immunoreactivity was visualized with 0.05% 3, 3'-diaminobenzidine (Sigma) and 0.03% H_2O_2. Counterstaining of nuclei was performed with Mayer's hematoxylin. A negative control for immunohistochemical staining was established by using the same concentration of normal rabbit IgG. CD31-positive vessels were counted in 5 fields of a matrigel plug section at 400× magnification under a microscope. Microvessel density (MVD) was expressed as the number of microvessels per square millimeter.

5. HMGB1-heparin binding assay.

Heparin-Sepharose CL-6B (GE Healthcare) equilibrated with PBS (10μl gel bed) was added to 200μl of HMGB1 (400μg/ml in PBS) solution and incubated

for 16h at 4℃ with gentle shaking. The reaction mixture was centrifuged at 8,000×g for 10min at 4℃. The supernatant was collected, and the Sepharose was washed with PBS three times. The supernatant and the resultant Sepharose gel samples were analyzed by SDS-PAGE to examine the binding of HMGB1 to heparin.

6. HMGB1 digestion assay.

Ten μl of HMGB1 (500μg/ml in PBS) was mixed with 2.5μl of heparin (32 or 320μg/ml) or PBS and incubated for 16h at 4℃. Additionally, the mixtures were mixed with 2.5μl of plasmin (20μg/ml) (Merck) and incubated for 1h at 25℃. The reaction mixtures were analyzed by SDS-PAGE.

7. Determination of HMGB1 levels in matrigel using Western blotting.

A matrigel mixture containing PBS, HMGB1 (2.5μg/ml, 100nM) or heparin (320μg/ml, 64units/ml)+HMGB1 was injected subcutaneously into the backs of mice. After 1, 3 or 10 days, the matrigel plugs were recovered. Matrigel homogenate corresponding to 2.5mg wet weight was electrophoresed on polyacrylamide gel (12.5%). The samples were electrophoretically blotted on polyvinylidine difloride membrane (Bio-rad, Hercules, CA, USA) at 45 V for 2h by a transblot apparatus. After the membrane was stained by ponceau S, it was incubated with 10% skim milk for 1h and was incubated overnight at 4℃ with mouse monoclonal anti-human HMGB1 antibody (R&D Systems, Minneapolis, MN, USA). After washing, the membrane was incubated with anti-mouse IgG goat polyclonal IgG-HRP (MBL, Nagoya, Japan) for 1h. The signals were finally visualized using an enhanced chemiluminescence system (Pierce Biotechnology, Rockford, IL, USA).

8. RT-PCR.

Total RNA was isolated from the mouse skin surrounding the matrigel plug using an RNeasy fibrous tissue mini kit (Qiagen, Hilden, Germany) (Fig. 1C). Complementary DNA was synthesized with a Takara RNA PCR kit Ver. 3.0 (Takara Bio, Nagahama, Japan) according to the manufacturer's instructions. The PCR reaction was performed in a PCR Thermal Cycler (Takara Bio) using Ex Taq DNA polymerase HS (Takara Bio), and sequence-specific primers (Table 1) according to the following program: after the initial denaturation at 94℃ for 3min, amplification was done using X cycles of 94℃ for 30 sec, Y℃ for 30 sec, and 72℃ for 60 sec, followed by a final extension at 72℃ for 7min (X and Y are defined in

Table 1 Primer sequences, annealing temperatures, amplification cycles and product sizes for RT-PCR

Primer		Sequence 5'-3'	Amplification cycles (X)	Annealing temperature (Y)	Product size
GAPDH	forward	ACCACAGTCCATGCCATCAC	27	55°C	452bp
	reverse	TCCACCACCCTGTTGCTGTA			
TNF-α	forward	TTCTGTCTACTGAACTTCGG	37	55°C	354bp
	reverse	GTATGAGATAGCAAATCGG			
iNOS	forward	GCTTAGAGAACTCAACCAC	37	55°C	454bp
	reverse	GCTGCCCTCGAAGGTGAGC			
eNOS	forward	CTGGACACCAGGACAACC	37	55°C	460bp
	reverse	GCTGCTGTGCGTAGCTCT			
MMP-2	forward	CCGTGGATGATGCTTTTGC	30	55°C	319bp
	reverse	CTGTATTCCCGACCGTTGA			
MMP-9	forward	TGCGCCACCACAGCCAAC	35	60°C	399bp
	reverse	GCCACGACCATACAGATAC			
VEGFR-1	forward	TGTGGAGAAACTTGGTGACCT	35	55°C	505bp
	reverse	TGGAGAACAGCAGGACTCCTT			
VEGFR-2	forward	AAGTGATTGAGGCAGACGCT	37	55°C	524bp
	reverse	TGATGCCAAGAACTCCAT			
bFGF	forward	GACCCCAAGCGGCTCTACTGC	35	55°C	298bp
	reverse	GTGCCACATACCAACTGGAGT			
VEGF-A	forward	GCGGGCTGCCTCGCAGT	37	55°C	$VEGF\text{-}A_{120}$ 275bp
	reverse	TCACCGCCTTGGCTTGTCA			$VEGF\text{-}A_{164}$ 407bp
					$VEGF\text{-}A_{188}$ 479bp

Table 1). The PCR product was analyzed by electrophoresis on 2% agarose gel.

9. Real-time quantitative PCR.

Real-time PCR was performed with a Light Cycler (Roche, Basel, Switzerland) according to the manufacturer's instructions. Reaction mixtures contained cDNA template, SYBR premix Ex Taq (Takara Bio, Shiga, Japan), and sequence-specific primers (Table 2).

10. Statistical analysis.

All data are presented as the means ± SEM. Differences between 2 groups were determined by ANOVA followed by Student's *t*-test. P values < 0.05 were considered statistically significant.

Results

The effect of HMGB1 and heparin on angiogenesis in a matrigel plug assay. The matrigel mixture was injected subcutaneously into the backs of mice as shown in Fig. 1. After 10 days, the matrigel plugs were recovered as shown in Fig. 2. It has been reported that 50 nuclei in the muscle tissue contain ~ 25 pg HMGB1 [32] and that LPS (100 ng/ml)-stimulated RAW264.7 cells (5×10^6 cells) release 10 μg HMGB1 into the culture medium [6]. Given that an individual cell has a volume of 10 μm^3 and 10% of the reported HMGB1 values represent extracellular release, the estimated concentration of HMGB1 in the tissues will be 0.05 (muscle tissue) and 0.2 (RAW264.7 cells) mg/ml, respectively. The concentrations of HMGB1 used in the present matrigel assay (2.5 μg/ml, 100 nM) corresponded to 5% and 1.25% of these estimated values, which would be readily attainable percentages under *in vivo* conditions in an inflammation area. The concentration of heparin (320 μg/ml, 64 units/ml) was determined according to the reports of Passaniti *et al.* [33] and Isaji *et al.* [34], who used FGF and VEGF as angiogenic growth factors, respectively. In the present study, angiogenesis did not appear to be induced in the phosphate-buffered saline (PBS) control group. Also in the groups treated with HMGB1 alone, the matrigel did not show any change compared with the PBS control. In the

Table 2 Primer sequences, annealing temperatures and product sizes for real-time PCR

Primer		Sequence 5'-3'	Annealing temperature	Product size
GAPDH	forward	TGACGTGCCGCCTGGAGAAA	55°C	98 bp
	reverse	AGTGTAGCCCAAGATGCCCTTCAG		
TNF-α	forward	GACCCTCACACTCAGATCATCCTTCT	55°C	106 bp
	reverse	GCGCTGGCTCAGCCACTC		
iNOS	forward	GGCAGCCTGTGAGACCTTTG	55°C	72 bp
	reverse	GCATTGGAAGTGAAGCGTTTC		
eNOS	forward	CAACGCTACCACGAGGACATT	55°C	90 bp
	reverse	CTCCTGCAAAGAAAAGCTCTGG		
MMP-2	forward	CCCCGATGCTGATACTGA	55°C	152 bp
	reverse	CTGTCCGCCAAATAAACC		
MMP-9	forward	GCCCTGGAACTCACACGACA	55°C	85 bp
	reverse	TTGGAAACTCACACGCCAGAAG		
VEGFR-1	forward	GGCAGACCAATACAATCCTAGATG	55°C	140 bp
	reverse	ACCAGGGTAATTCCAGCTCATTT		
VEGFR-2	forward	CGACATAGCCTCCACTGTTTATG	55°C	109 bp
	reverse	TTTGTTCTTGTTCTCGGTGATGT		
bFGF	forward	CCCACCAGGCCACTTCAA	55°C	71 bp
	reverse	GATGGATGCGCAGGAAGAA		
VEGF-A_{120}	forward	GCCAGCACATAGAGAGAATGAGC	55°C	104 bp
	reverse	CGGCTTGTCACATTTTTCTGG		
VEGF-A_{164}	forward	GCCAGCACATAGAGAGAATGAGC	55°C	97 bp
	reverse	CAAGGCTCACAGTGATTTTCTGG		
VEGF-A_{188}	forward	GCCAGCACATAGAGAGAATGAGC	55°C	171 bp
	reverse	AACAAGGCTCACAGTGAACGCT		

heparin-treated group, there was a low level of angiogenesis, judging from the macroscopic color change. In the group treated with the combination of HMGB1 and heparin, the whole gel had red color heavily, and a lot of the blood vessels seemed to be elongated into the center of the matrigel (Fig. 2A). Next, we determined the hemoglobin contents in the matrigel isolated from the back. We obtained consistent results that reflected the color changes described above. In the PBS or HMGB1 group, little hemoglobin was detected in the matrigel. In the heparin group, there was a small amount of hemoglobin detected in the gel. In the group treated with the combination of HMGB1 and heparin, the hemoglobin content was significantly increased (Fig. 2B). Taken together, these results indicate that angiogenesis was induced by the combination of HMGB1 and heparin in the matrigel plug assay. Ten days after inoculation, a thin section of the matrigel was stained with hematoxylin-eosin (HE) (Fig. 3). In the group treated with the combination of HMGB1 and heparin, many infiltrating cells, including leukocytes, were observed in the gel (Fig. 3A, panel d). However, few cells were observed in the gel sections from other groups (Fig. 3A, panels a-c). Secondly, immunostaining was performed with an antibody against CD31 that is a marker antigen of vascular endothelial cells. Many cells with strong positively for CD31 were seen to be forming luminal structures in the sections from matrigels treated with the combination of HMGB1 and heparin (Fig. 3A, panel h). The staining with anti-CD31 antibody was specific, because staining with the control antibody did not reveal any structures in the same section. In other groups, few CD31-positive structures were observed (Fig. 3A, panels e-g). The number of CD31-positive luminal structures was counted in five random fields. In the group treated with HMGB1 and heparin, the number of CD31-positive luminal structures was significantly increased in comparison with the number by treatment with HMGB1 or heparin alone (Fig. 3B). Taken together, these results showed that the combination of HMGB1 and heparin induced the migration of vascular endothelial cells, leading to the formation of new vessels in the matrigel.

HMGB1 binds to heparin. SDS-PAGE analysis following the incubation of HMGB1 with heparin-Sepharose gel revealed that HMGB1 was present in the heparin-Sepharose gel fraction but not in the supernatant fraction, indicating that HMGB1 formed a complex with heparin (Fig. 4A).

Degradation of HMGB1 by plasmin in the presence or absence of heparin. It has been reported that HMGB1 is a good substrate for plasmin [35]. Therefore, we examined whether the complex formation between HMGB1 and heparin affected the digestion efficiency by plasmin. As shown in Fig. 4B, HMGB1 was resistant to plasmin digestion in the presence of heparin. Even at a lower concentration (32μg/ml: 1/10 the concentration of heparin used in the matrigel assay), the presence of heparin inhibited the degradation of HMGB1 by plasmin.

The determination of HMGB1 levels in matrigel. A matrigel mixture containing PBS, HMGB1 or heparin + HMGB1 was injected subcutaneously into the backs of mice. After 1, 3 or 10 days, the mice were sacrificed and the matrigel plugs were recovered. HMGB1 was detected by Western blotting with anti-HMGB1 monoclonal antibody. An equivalent amount of matrigel homogenate, corresponding to 2.5mg wet weight, was loaded on each lane (Fig. 5A). In the group treated with HMGB1 and heparin, HMGB1 disappeared completely from the matrigels 3 days after inoculation, whereas there was no marked change in HMGB1 level in the group treated with HMGB1 alone throughout the 10-day measurement period (Fig. 5B).

The expression of angiogenesis-related mRNA in the mouse skin surrounding the matrigel plug. Total RNA was extracted from mouse skin surrounding the matrigel plug. Ten days after the inoculation of matrigel, RT-PCR for TNF-α, inducible nitric oxide synthase (iNOS), endothelial nitric oxide synthase (eNOS), MMP-2, MMP-9, VEGF receptor-1 (VEGFR-1), VEGFR-2, basic fibroblast growth factor (bFGF) and VEGF-A was performed with extracted RNA, and the band density of each group was compared after agarose gel electrophoresis. The TNF-α mRNA level was higher in the HMGB1 group than the PBS group. The TNF-α mRNA level was significantly higher in the group treated with HMGB1 and heparin than in that treated with HMGB1 alone. The expression of TNF-α mRNA in the other groups was minimal under the same PCR conditions. There were no significant differences in iNOS, eNOS, MMP-2, MMP-9, VEGFR-1, VEGFR-2 or bFGF mRNA levels among the groups.

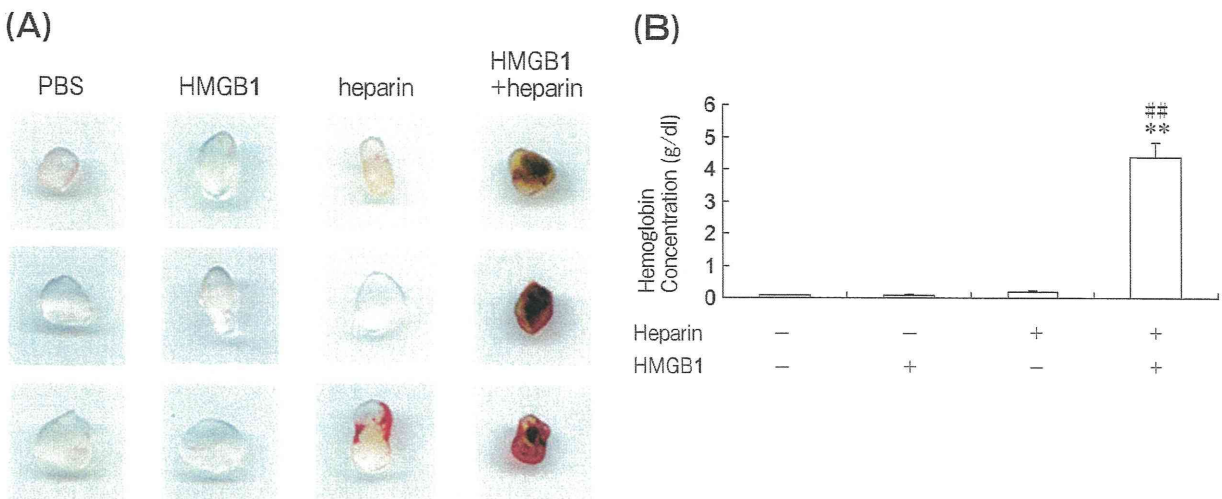

Fig. 2 Effect of HMGB1 and heparin on angiogenesis in the matrigel assay. (A) A matrigel mixture containing HMGB1 and heparin alone or in combination was injected subcutaneously into the backs of mice. After 10 days, the matrigel plugs were recovered. Each group consisted of 6 mice. Three representative cases are shown. (B) The concentrations of hemoglobin in the matrigel plugs were determined. The results are the means ± SEM of 6 matrigels. $^{**}P<0.01$ compared with the PBS control group without any treatment. $^{\#\#}P<0.01$ compared with the group treated with heparin alone.

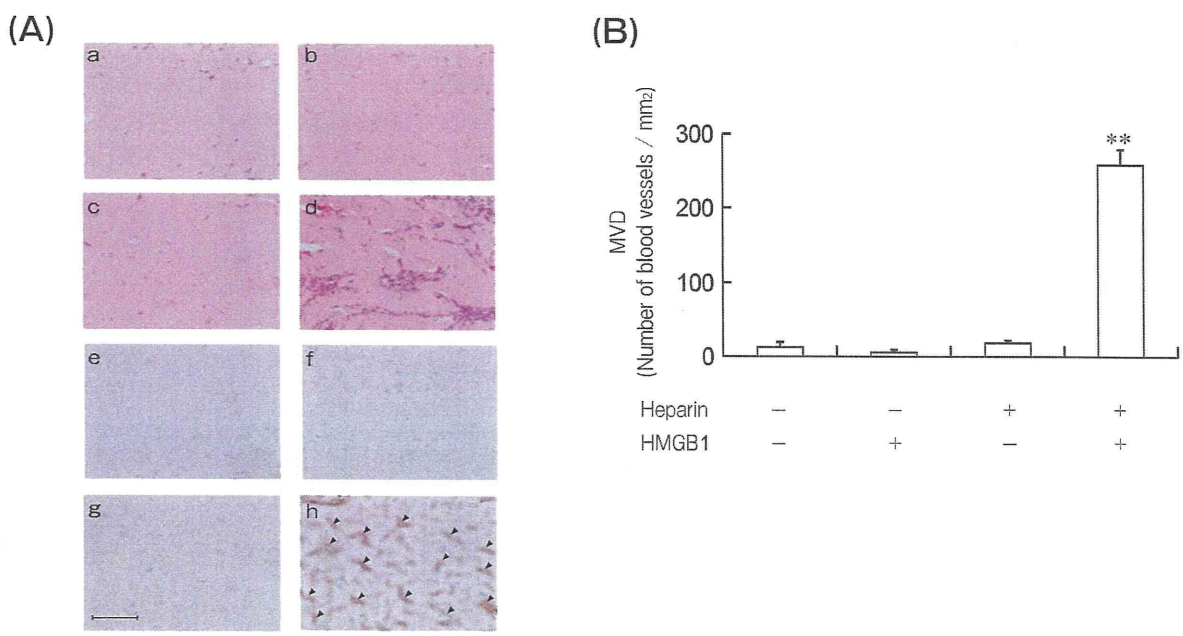

Fig. 3 Histological study of matrigel plugs. (A) The matrigels were removed from the mouse back 10 days after inoculation and fixed in 10% formalin. Paraffin-embedded sections of matrigel plug were stained by hematoxylin-eosin (a-d) and by anti-CD31 antibody (e-h). The matrigels contained PBS (a, e), HMGB1 alone (b, f), heparin alone (c, g), or a combination of HMGB1 and heparin (d, h). Arrowheads indicate CD31-positive blood vessels. The scale bar represents 100 μm. (B) CD31-positive vessels were counted in 5 fields of the matrigel plug section at 400 × magnification under a microscope. The microvessel density (MVD) was expressed as the number of microvessels per square millimeter. The results are the means ± SEM of 5 fields. $^{**}P<0.01$ compared with the PBS control group.

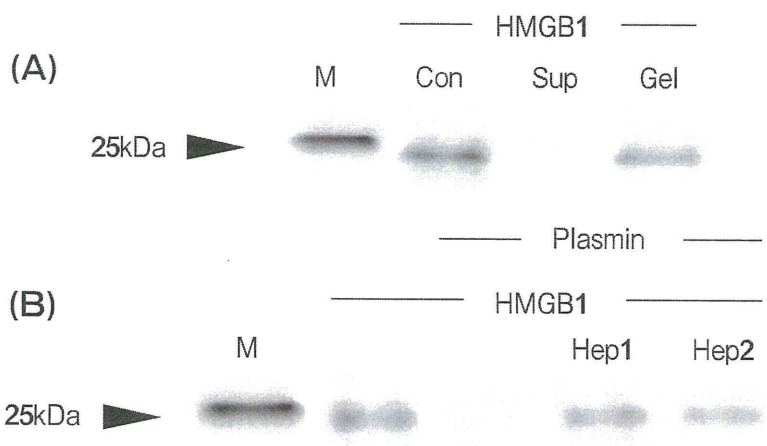

Fig. 4 HMGB1 binding to heparin and its effect on digestion by plasmin. (A) HMGB1 was mixed with heparin-Sepharose and incubated for 16h at 4°C. After incubation, the supernatant (Sup) and the protein from the heparin-Sepharose gel (Gel) were electrophoresed on 12% SDS-PAGE gel under a reducing condition, followed by staining with Coomassie-blue. (M) is a molecular weight marker. (Con) represents the HMGB1 control. (B) HMGB1 was preincubated with or without heparin for 16h at 4°C. After preincubation, the mixtures were subjected to plasmin digestion for 1h at 25°C. The resultant mixtures were electrophoresed and the gels were stained as mentioned above. (Hep1) is HMGB1 incubated with 32μg/ml heparin and plasmin. (Hep2) is HMGB1 incubated with 320μg/ml heparin and plasmin.

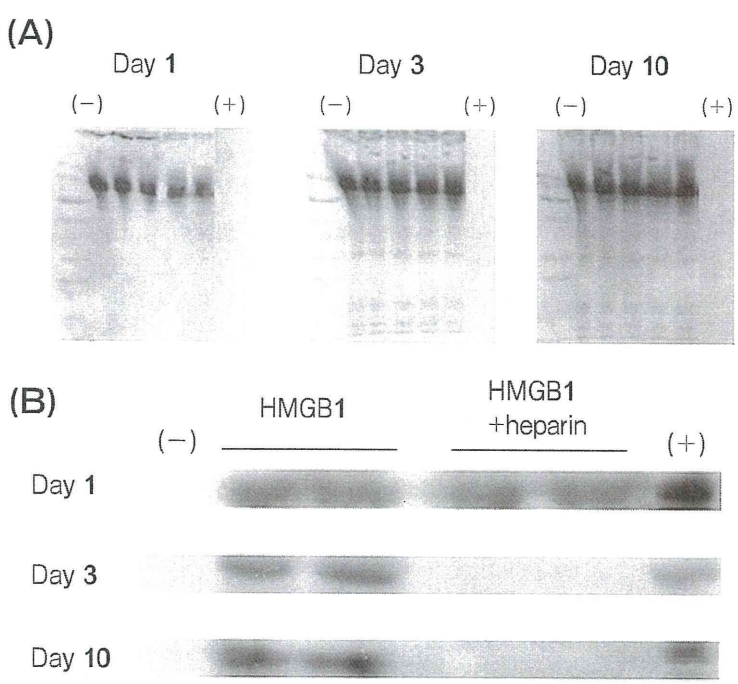

Fig. 5 Determination of HMGB1 levels in matrigel using Western blotting. A Matrigel mixture containing PBS, HMGB1 (2.5μg/ml, 100nM) or heparin (320μg/ml, 64units/ml) + HMGB1 was injected subcutaneously into the backs of mice. After 1, 3 and 10 days, the matrigel plugs were recovered. The matrigel plugs were homogenized and an amount of homogenate corresponding to 2.5mg wet weight of matrigel was loaded on each lane. (A) Ponseau S staining of the PVDF membrane. (B) Detection of HMGB1 in matrigel. (−) negative control; matrigel contains PBS alone. (+) positive control; recombinant human HMGB1.